NUREG/CR-3660, Vol. 2
UCID-19988, Vol. 2

Probability of Pipe Failure in the Reactor Coolant Loops of Westinghouse PWR Plants

Volume 2: Pipe Failure Induced by Crack Growth

Load Combination Program

H. H. Woo, R. W. Mensing, B. J. Benda

Prepared for
U.S. Nuclear Regulatory Commission

Lawrence
Livermore
National
Laboratory

NOTICE

Availability of Reference Materials Cited in NRC Publications

Most documents cited in NRC publications will be available from one of the following sources:

1. The NRC Public Document Room, 1717 H Street, N.W.
   Washington, DC 20555
2. The NRC/GPO Sales Program, U.S. Nuclear Regulatory Commission,
   Washington, DC 20555
3. The National Technical Information Service, Springfield, VA 22161

Although the listing that follows represents the majority of documents cited in NRC publications, it is not intended to be exhaustive.

Referenced documents available for inspection and copying for a fee from the NRC Public Document Room include NRC correspondence and internal NRC memoranda; NRC Office of Inspection and Enforcement bulletins, circulars, information notices, inspection and investigation notices; Licensee Event Reports; vendor reports and correspondence; Commission papers; and applicant and licensee documents and correspondence.

The following documents in the NUREG series are available for purchase from the NRC/GPO Sales Program: formal NRC staff and contractor reports, NRC sponsored conference proceedings, and NRC booklets and brochures. Also available are Regulatory Guides, NRC regulations in the *Code of Federal Regulations*, and *Nuclear Regulatory Commission Issuances*.

Documents available from the National Technical Information Service include NUREG series reports and technical reports prepared by other federal agencies and reports prepared by the Atomic Energy Commission, forerunner agency to the Nuclear Regulatory Commission.

Documents available from public and special technical libraries include all open literature items, such as books, journal and periodical articles, and transactions. *Federal Register* notices, federal and state legislation, and congressional reports can usually be obtained from these libraries.

Documents such as theses, dissertations, foreign reports and translations, and non-NRC conference proceedings are available for purchase from the organization sponsoring the publication cited.

Single copies of NRC draft reports are available free, to the extent of supply, upon written request to the Division of Technical Information and Document Control, U.S. Nuclear Regulatory Commission, Washington, DC 20555.

Copies of industry codes and standards used in a substantive manner in the NRC regulatory process are maintained at the NRC Library, 7920 Norfolk Avenue, Bethesda, Maryland, and are available there for reference use by the public. Codes and standards are usually copyrighted and may be purchased from the originating organization or, if they are American National Standards, from the American National Standards Institute, 1430 Broadway, New York, NY 10018.

GPO Printed copy price

NUREG/CR-3660, Vol. 2
UCID-19988, Vol. 2
RM

Probability of Pipe Failure in the Reactor Coolant Loops of Westinghouse PWR Plants

Volume 2: Pipe Failure Induced by Crack Growth

Load Combination Program

Manuscript Completed: January 1984
Date Published: August 1984

Prepared by
H. H. Woo, R. W. Mensing, and B. J. Benda

Lawrence Livermore National Laboratory
7000 East Avenue
Livermore, CA 94550

Prepared for
Division of Engineering Technology
Office of Nuclear Regulatory Research
U.S. Nuclear Regulatory Commission
Washington, D.C. 20555
NRC FIN No. A0133

The NUREG/3660 report series, "Probability of Pipe Failure in the Reactor Coolant Loops of Westinghouse PWR Plants," contains four volumes:

Volume 1: Summary
Volume 2: Pipe Failure Induced by Crack Growth
Volume 3: Guillotine Break Indirectly Induced by Earthquakes
Volume 4: Pipe Failure Induced by Crack Growth, West Coast Plants

ABSTRACT

This report assesses the probability of reactor coolant loop (RCL) piping failures resulting from a crack growth mechanism. The Westinghouse pressurized water reactor (PWR) plants in the United States east of the Rocky Mountains are considered. After the introduction (Section 1), the assessment is presented in five parts (Sections 2-6). Section 2 describes the characteristics of RCL piping in these Westinghouse PWR plants. Section 3 describes the methodology used in the analysis. Sections 4 and 5 present the best-estimate and uncertainty analyses, respectively. Our conclusions are presented in Section 6, along with recommended items for consideration in future licensing regulations.

CONTENTS

LIST OF FIGURES

LIST OF TABLES

ACKNOWLEDGMENTS

This work was funded by the Mechanical/Structural Engineering Branch, in the Office of Nuclear Regulatory Research of the U.S. Nuclear Regulatory Commission. Dr. J. O'Brien was the technical monitor of the work.

The authors wish to express their appreciation to C. K. Chou of Lawrence Livermore National Laboratory for guidance, and to R. A. Holmes, E. R. Johnson, and T. C. Esselman of the Water Reactor Division of Westinghouse Electric Corporation for their cooperation in providing the design data package for our analyses.

Our peer-review panel included E. C. Rodabaugh, Chairman (retired from Battelle Columbus Laboratories), Dr. S. H. Bush (Review & Synthesis Associates), and Prof. A. C. Cornell (Stanford University). We appreciate their reviews, comments, and suggestions.

The authors acknowledge the contributions from our consultants; Dr. D. O. Harris of Failure Analysis Associates, and D. F. Landers of Teledyne Engineering Services.

Thanks are also extended to L. L. George for developing the methodology for the system piping failure probability calculations, to G. S. Holman for encouragement, to S. D. Greenberg and T. R. Nelson for editorial help, and to T. Dwinell and P. Ruiz for typing the draft manuscripts.

PROBABILITY OF PIPE FAILURE IN THE REACTOR COOLANT LOOPS
OF WESTINGHOUSE PWR PLANTS
Volume 2: Pipe Failure Induced by Crack Growth

EXECUTIVE SUMMARY

The Code of Federal Regulations requires that structures, systems, and components affecting the safe operation of nuclear power plants be designed to withstand combinations of loads from natural phenomena, normal operating conditions, and postulated accidents. One of the mandated requirements for load combinations concerns the coupled effects of a safe shutdown earthquake (SSE) and a loss of coolant accident (LOCA). This requirement has been the subject of controversy because both events have very low probabilities of occurring. The issue has become more controversial in recent years because the postulated LOCA and SSE loads have each been increased by a factor of two or more (to account for such phenomena as asymmetric blowdown in pressurized water reactors), and because better techniques for defining loading have been developed.

The Load Combination Program, initiated at Lawrence Livermore National Laboratory (LLNL) in 1980, aims to provide the U.S. Nuclear Regulatory Commission (NRC) with a technical basis for solving load combination issues in nuclear power plant designs. One of the program's tasks is to determine whether the requirement to consider the load of a large LOCA combined with that of an SSE is justified for the safe operation of nuclear power plants.

In attacking the problem, LLNL has adopted a probabilistic approach to estimate the probability that large LOCA and SSE loads will occur simultaneously, and to estimate the probability that a large LOCA will be caused only by normal and abnormal loading conditions (without an earthquake). These estimates give us useful information on the likelihood of an asymmetric blowdown, which would be part of a large LOCA.

The first phase of the Load Combination Program was a pilot study on the reactor coolant loop (RCL) piping of the Zion Unit 1 plant. The study was divided into two cases, according to the postulated cause of failure. One case was concerned with pipe failure caused by crack growth in the pipe weld joint locations. The second case dealt with causes other than the crack growth mechanism, such as the failure of support systems. The pilot study's results indicated that the probabilities for a failure due to the simultaneous occurrence of an SSE and a double-ended guillotine break (DEGB), resulting from either cause, were extremely low. For convenience, we refer to the first case as a direct DEGB; the second case is referred to as an indirect DEGB. In this volume of the report, we address only the case of a direct DEGB.

The major objective of this report is to provide an estimate of the probability of a direct DEGB occurring, due to the fatigue crack growth mechanism in the RCL piping at the Westinghouse pressurized water reactor (PWR) plants east of the Rocky Mountains. Seventeen sample plants, representing 33 reactors at 19 sites, were selected to represent the larger population of Westinghouse PWR plants in the region under consideration. For Westinghouse PWR plants west of the Rocky Mountains, a similar study is documented in Volume 4 of this report series.

Two analyses, a best-estimate analysis and an uncertainty analysis, were performed. The former gives a point estimate of the probability of a failure, while the latter provides confidence bounds for this estimate.

In the best-estimate analysis, we followed the methodology developed in the pilot study, and made point estimates of the probabilities for an RCL piping failure at each of the 17 sample plants. For these plants, leakage estimates ranged from 10^{-8} to 10^{-9} per plant year. The probabilities for a direct DEGB in the RCL were estimated as being about 10^{-12} per plant year. In the uncertainty analysis, we developed a methodology that incorporates uncertainties in several parameters affecting the assessments of DEGB probabilities. The confidence bounds for the 90th percentiles of the probabilities for a leak and a direct DEGB were estimated as 2.4×10^{-7} and 7.5×10^{-11} per plant year, respectively. Based on the results of both analyses, we concluded:

(1) A direct DEGB is a very unlikely event for the RCL piping in Westinghouse PWR plants east of the Rocky Mountains.

(2) Earthquakes contribute very little (at most about 1%) to the probability of a direct DEGB in the RCL piping of the Westinghouse PWR plants east of the Rocky Mountains.

(3) The difference of at least three orders of magnitude between the leak and the direct DEGB probabilities suggests that a leak is more likely than a direct DEGB in the RCL piping for Westinghouse PWR plants east of the Rocky Mountains.

These conclusions have led us to the following considerations for design criteria for the RCL piping in Westinghouse PWR plants east of the Rocky Mountains:

(1) The design requirements for simultaneous DEGB and SSE loads (as related to the crack growth mechanism in the RCL piping) should be reconsidered, since the probabilities that these events will occur are extremely low.

(2) The design requirements for postulating crack growth mechanism failure modes in the RCL piping should focus on the "leak" mode rather than on the "DEGB" mode.

1. INTRODUCTION

1.1 Background

The Code of Federal Regulations requires that structures, systems, and components affecting the safe operation of nuclear power plants be designed to withstand those combinations of loads that can be expected from natural phenomena, normal operating conditions, and postulated accidents.[1] An example of a load combination requirement for nuclear plants is the effect of a safe shutdown earthquake (SSE) load coupled with the load from a loss of coolant accident (LOCA). In a recent evaluation, these combined loads were increased by a factor of two or more to account for such phenomena as asymmetric blowdown in a pressurized water reactor (PWR). The U.S. Nuclear Regulatory Commission (NRC) recognized the urgent need for resolving this issue, since implementing the regulations have resulted in design and construction difficulties, increased construction costs, increased radiation exposure of maintenance crews, and a reduced reliability for the stiffer systems under normal operating transients.

In response to a request from the NRC, Lawrence Livermore National Laboratory (LLNL) undertook a multiyear Load Combination Program, beginning in fiscal year 1980. The first phase of this program was to assess the influence of seismic loads on a double-ended guillotine break (DEGB) event in the reactor cooling loop (RCL) piping of a PWR plant. A probabilistic approach was adopted for the evaluation. The results of that assessment indicated:

(1) Fatigue crack growth from all transients, including earthquakes, would be an extremely unlikely mechanism for inducing a DEGB.

(2) The contribution of earthquakes to the occurrence of this unlikely event would be a small percentage of the probability for a total failure.[2]

However, the estimate for the probability of a failure used in that study was a point estimate, since uncertainties in the input variables were not considered.

In this study, therefore, we performed both a best-estimate analysis, and an uncertainty analysis to provide the uncertainty bounds for the estimated failure probabilities. Furthermore, our study covered a large population of Westinghouse PWR plants (33 reactor units at 19 plant sites) located east of the Rocky Mountains.

1.2 Objectives and Contents of this Report

The two main objectives of this report are to present the results from analyzing the probability that RCL piping failures might be induced by fatigue crack growth, and to recommend action items for future licensing regulations on the load combination requirements for the RCL piping in Westinghouse PWR plants east of the Rocky Mountains.

This report consists of six sections and an Appendix. Section 1 is the Introduction. Section 2 describes the characteristics of the RCL piping in Westinghouse PWR plants. Section 3 gives an overview of the analytical methodology. Section 4, the best-estimate analysis, gives a point estimate for the probability of a failure in the RCL piping for each of the plants. Section 5 presents an uncertainty analysis, which provides the uncertainty bounds for the plant with the highest probability of a DEGB failure, as indicated by the best-estimate analysis. Section 6 lists the study's conclusions, and recommends action items for consideration in future licensing regulations. Appendix A tabulates information regarding the RCL pipe geometries and loadings as derived from the Westinghouse data package.

2. REACTOR COOLANT LOOP (RCL) DESCRIPTIONS FOR THE WESTINGHOUSE PWR PLANTS EAST OF THE ROCKY MOUNTAINS

2.1 General Information

The primary components of the Westinghouse PWR nuclear steam supply system (NSSS) are the reactor vessel, steam generators, and the reactor coolant pumps. Figure 1 shows a typical four-loop NSSS supplied by Westinghouse. The piping for each reactor coolant loop (RCL) contains a hot leg (reactor pressure vessel [RPV] to steam generator [SG]), a crossover leg (steam generator to reactor coolant [RC] pump), and a cold leg (reactor coolant pump to reactor pressure vessel). Westinghouse also supplies 2-loop and 3-loop configurations. Figure 2 shows the locations of the 16 circumferential girth butt welds that are common to each loop, which are the concern of this study.

Although the general arrangement of the Westinghouse RCL system has not changed since 1961, the designs for the steam generators and the loop piping differ in the piping materials and the number of loops used, and in their geometries. Table 1 lists Westinghouse reactors in the U.S. that are in operation, under construction, or on order, as of August 1983.[3,4]

2.2 The PWR Plants Being Considered

Westinghouse has provided the Load Combination Program with a design data package covering 36 (out of a total of 59)[4] reactor units at 21 plant sites, including 2 sites on the west coast.

In this volume of the report, we are concerned with the Westinghouse reactor units located east of the Rocky Mountains. A similar study of the west coast plants is presented in Volume 4 of this report series. Furthermore, since many reactor units have identical designs, for our analysis we identified 17 sample plants which are representative of 33 reactor units and 19 plant sites. The design data for one sample plant may thus represent more than one reactor unit and more than one plant site.

Table 2 summarizes the characteristics of the RCLs in the Westinghouse plants under consideration. The RCLs in these plants vary in steam generator design (four models, as shown in Table 3), number of loops per unit (two, three, or four loops), method of pipe manufacture (cast or forged), pipe material (four types), and wall thicknesses for the girth butt welds (two classes). We believe that the 17 sample plants chosen for analysis represent the generic characteristics of Westinghouse RCLs.

2.3 Design Data Package

Westinghouse provided a design data package for the 17 sample plants containing relevant information about the pipe material, pipe geometry, and the design loadings. These loadings consist of internal pressure in the pipe, the dead weight, loads resulting from the restraint of thermal expansion, and seismic loads. Appendix A tabulates the pipe geometries and design loadings at each of the 16 welds in the RCL piping of the 17 sample plants.

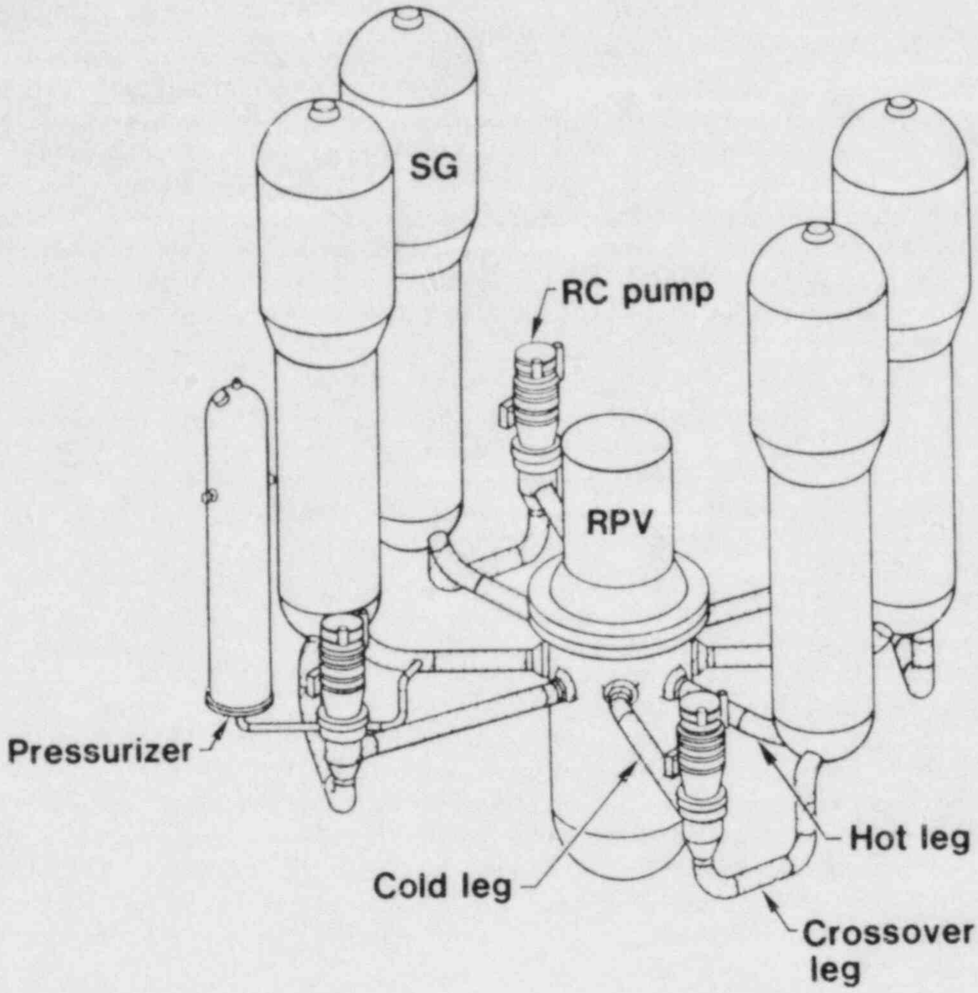

Figure 1. A Typical Westinghouse nuclear steam supply system (NSSS).

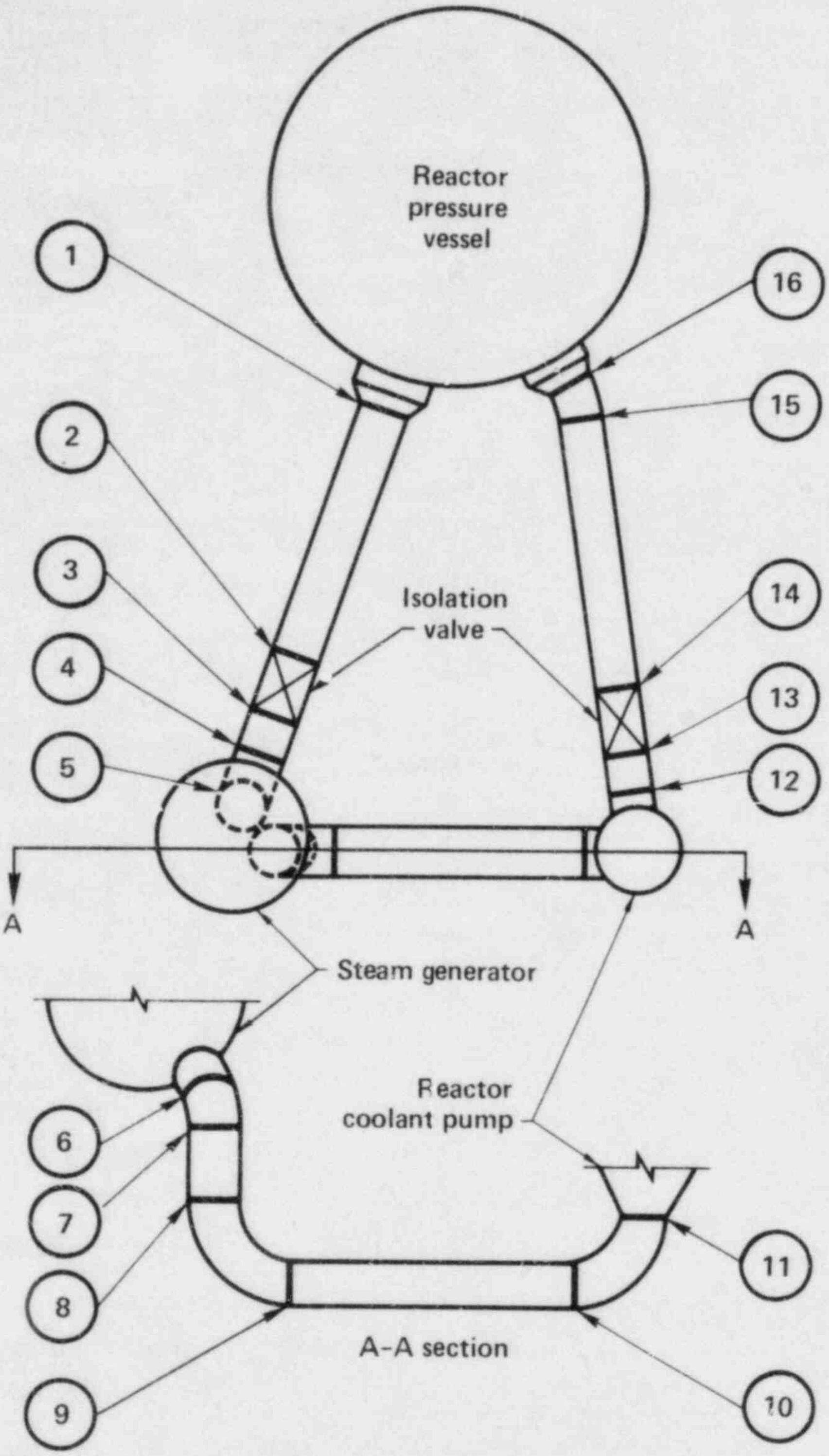

Figure 2. The locations of the 16 circumferential weld joints in the reactor coolant loop (RCL) piping.

Table 1. Characteristics of the reactor coolant loops (RCLs) for all Westinghouse PWR plants in the U.S.

Plant name	Steam generator model[a]	Number of loops	Method of pipe manufacture	Pipe material type[b]	Pipe wall thickness type[c]	Commercial operation
Yankee Rowe	13	4	--	--	F	6/61
San Onofre 1	27	3	Forged	1	E	1/68
Haddam Neck	27	4	Forged	3	E	1/68
Ginna	44	2	Forged	1	C	3/70
Point Beach 1 & 2	44	2	Forged	1	C	12/70, 10/72
Robinson 2	44	3	Forged	1	C	3/71
Turkey Point 3 & 4	44	3	Forged	1	C	12/72, 9/73
Indian Point 2 & 3	44	4	Forged	1	C	7/74, 8/76
Prairie Island 1 & 2	51	2	Forged	1, 5	C/D	12/73, 12/74
Kewaunee	51	2	Cast	5	D	6/74
Surry 1 & 2	51	3	Forged	1	C	12/72, 5/73
Farley 1 & 2	51	3	Cast	4	B	12/77, 7/81
Beaver Valley 1 & 2	51	3	Cast	4, 5	D/B	4/77, 86
North Anna 1 & 2	51	3	Cast	1	A	6/78, 12/80
Zion 1 & 2	51	4	Forged	1	C	10/73, 9/74
Diablo Canyon 1 & 2	51	4	Forged	1	C	--
Salem 1 & 2	51	4	Forged	1	C	6/77, 10/81
D. C. Cook 1 & 2	51	4	Cast	5	D	8/75, 7/78
Trojan	51	4	Cast	4	B	5/76
Sequoyah 1 & 2	51	4	Cast	5	B	7/81, 6/82
Virgil C. Summer 1	D	4	Forged	2	B	10/83
Shearon Harris 1 & 2	D	3	Forged	2	B	86, 90
Byron 1 & 2	D	3	Forged	2	B	84, 85
Braidwood 1 & 2	D	4	Forged	2	B	85, 86
Marble Hill 1 & 2	D	4	Forged	2	B	86, 87
McGuire 1 & 2	D	4	Cast	4	B	12/81, 10/83
Catawba 1 & 2	D	4	Cast	4	B	85, 87
Commanche Peak 1 & 2	D	4	Cast	4	B	84, 85
Watts Bar 1 & 2	D	4	Cast	4	B	84, 85
Seabrook 1 & 2	F	4	Forged	2	B	84, 87
Vogtle 1 & 2	F	4	Cast	4	B	87, 88
Millstone 3	F	4	Cast	4	B	86
Wolf Creek	F	4	Cast	4	B	84
Callaway 1	F	4	Cast	4	B	85
South Texas 1 & 2	E	4	Cast	4	B	86, 88

[a] This is the Westinghouse model designation.

[b] Five materials are used: 1 = ASTM-A376-316; 2 = SA-376-304N; 3 = SA-351-CF8A; 4 = SA-351-CF8M; 5 = SA-430-316.

[c] Pipe Wall Thicknesses

	Hot leg (29 in. I.D.)	Crossover leg (31 in. I.D.)	Cold leg (27.5 in. I.D.)
A	2.33	2.48	2.21
B	2.45	2.60	2.32
C	2.70	2.88	2.56
D	2.47[d]	2.59[e]	2.47
E	2.50[d]	2.56[e]	2.50
F	NA		

[d] 27.5 in. I.D.

[e] 29.0 in. I.D.

Table 2. Characteristics of reactor coolant loops for the Westinghouse plants under consideration east of the Rocky Mountains.

Sample plant number	Number of plant sites	Number of units	Number of loops per unit	Steam generator model[a]	Method of pipe manufacture	Pipe material type[b]	Class of wall thickness for weld[c]
1	1	1	2	51	Cast	4	TB
2	1	2	4	D	Cast	3	TA
3	1	2	4	51	Cast	4	TB
4	1	2	4	E	Cast	3	TA
5	1	2	4	D	Cast	3	TA
6	2	2	4	F	Cast	3	TA
7	1	2	4	51	Forged	1	TA
8	1	2	4	D	Forged	2	TA
9	1	2	2	51	Forged	1	TA
10	1	1	3	51	Cast	4	TA
11	1	2	4	51	Forged	1	TA
12	1	2	4	D	Cast	3	TB
13	1	1	3	D	Forged	2	TA
14	2	4	4	D	Forged	2	TA
15	1	2	3	D	Forged	2	TA
16	1	2	4	F	Forged	2	TA
17	1	2	3	51	Cast	3	TA

[a]This is the Westinghouse model designation.

[b]Pipe material type: 1 = ASTM-A376-316; 2 = SA-376-304N; 3 = SA-351-CF8A; 4 = SA-351-CF8M.

[c]For this table we have defined two classes (TA and TB) of wall thicknesses for the 16 girth-butt welds, so as to include all the pipe wall thicknesses noted in Table 1. Details can be found in Appendix A.

	Hot leg (in.)	Crossover leg (in.)	Cold leg (in.)
TA	2.45 - 3.375	2.6 - 3.3125	2.32 - 3.03
TB	2.8 - 3.375	3.0 - 3.3125	2.7 - 3.03

Table 3. A list of transients, and the postulated numbers of their occurrences over a 40-year plant life, for the Westinghouse steam generator designs.

Transients	Occurrences for steam generator model[a]			
	51	D	E	F
Heatup and cooldown (at 100°F/h)	200 each	200 each	200 each	200 each
Unit loading and unloading (at 5% of full power/minute)	18 300 each	13 200 each	13 200 each	13 200 each
Step load increase and decrease (at 10% of full power)	2 000 each	2 000 each	2 000 each	2 000 each
Large step load decrease (with steam dump)	200	200	200	200
Loss of load	80	80	80	80
Loss of power	40	40	40	40
Loss of flow (partial loss)	80	80	80	80
Reactor trip (from full power)	400	400	400	400
Steam line break	1	1	1	1
Turbine roll test	10	20	20	20
Hydrostatic test Condition	5	5	5	5

[a] Although the number of occurrences may be identical for different steam generator (SG) designs, the resulting temperature and pressure variations for each SG design may be different. SG Models 13, 27, and 44 are not shown. However, their effects on the temperature and pressure variations are similar to those of the SG designs that are listed.

3. METHODOLOGY USED IN THE ANALYSIS

3.1 Introduction

Our estimates for the probabilities of failure in the RCL piping welds were derived from a two-stage analysis: a best-estimate analysis and an uncertainty analysis. The best-estimate analysis provides a point estimate by using judgment in choosing the best available inputs and models. The uncertainty analysis considers the uncertainties associated with these inputs and models, and establishes the uncertainty bounds for the estimated probabilities of failure.

Both analyses start by estimating the probability for the occurrence of a failure at each vulnerable location in the RCL piping; that is, at the circumferential butt weld joints. In the following subsections, we present a brief description of the procedure used to estimate this probability for a single weld joint, followed by the procedures for estimating the probabilities for RCL systems. Finally, we discuss the details of both analyses.

3.2 Probability Estimates for a Weld Joint Failure

Failure at a weld joint is defined either as a leak or a DEGB. Figure 3 provides a computational flow chart showing how a piping reliability model is used to estimate the probability of failure at a weld joint. The model used is based on a probabilistic fracture mechanics concept. Details of the model's basic assumptions can be found in Reference 6.

The computations start by considering the probability that a crack exists in a weld. In the simulation process, a Monte Carlo method of numerical simulation is then used to start the selection of samples at a weld. The size of the initial population of crack-like defects at the weld are considered as being randomly distributed. These initial cracks have a certain probability of being detected and repaired during preservice inspection and hydrostatic proof testing. Repairing these cracks modifies the initial crack size distribution: the remaining cracks will grow by following a characteristic pattern of subcritical crack growth. Loading events consist of normal and abnormal operating conditions, and earthquakes.

For the 40-year life of the plant, the growth history is calculated for each crack sample. The critical sizes of cracks for which a leak or a DEGB will occur can be determined by applying the appropriate failure criteria. The probability of a leak or a DEGB at a weld joint during a given time interval is equal to the probability that a crack will grow to the corresponding critical size within that interval. A computer program, PRAISE (Piping Reliability Analysis Including Seismic Events), has been developed to carry out the detailed calculations.[7]

3.3 Probability Estimates for RCL System Piping Failure

After the failure probabilities for each weld joint have been obtained, they can be combined to estimate the possibility of failure in the RCL system piping.[8] In the present study, we define a system piping failure as being a

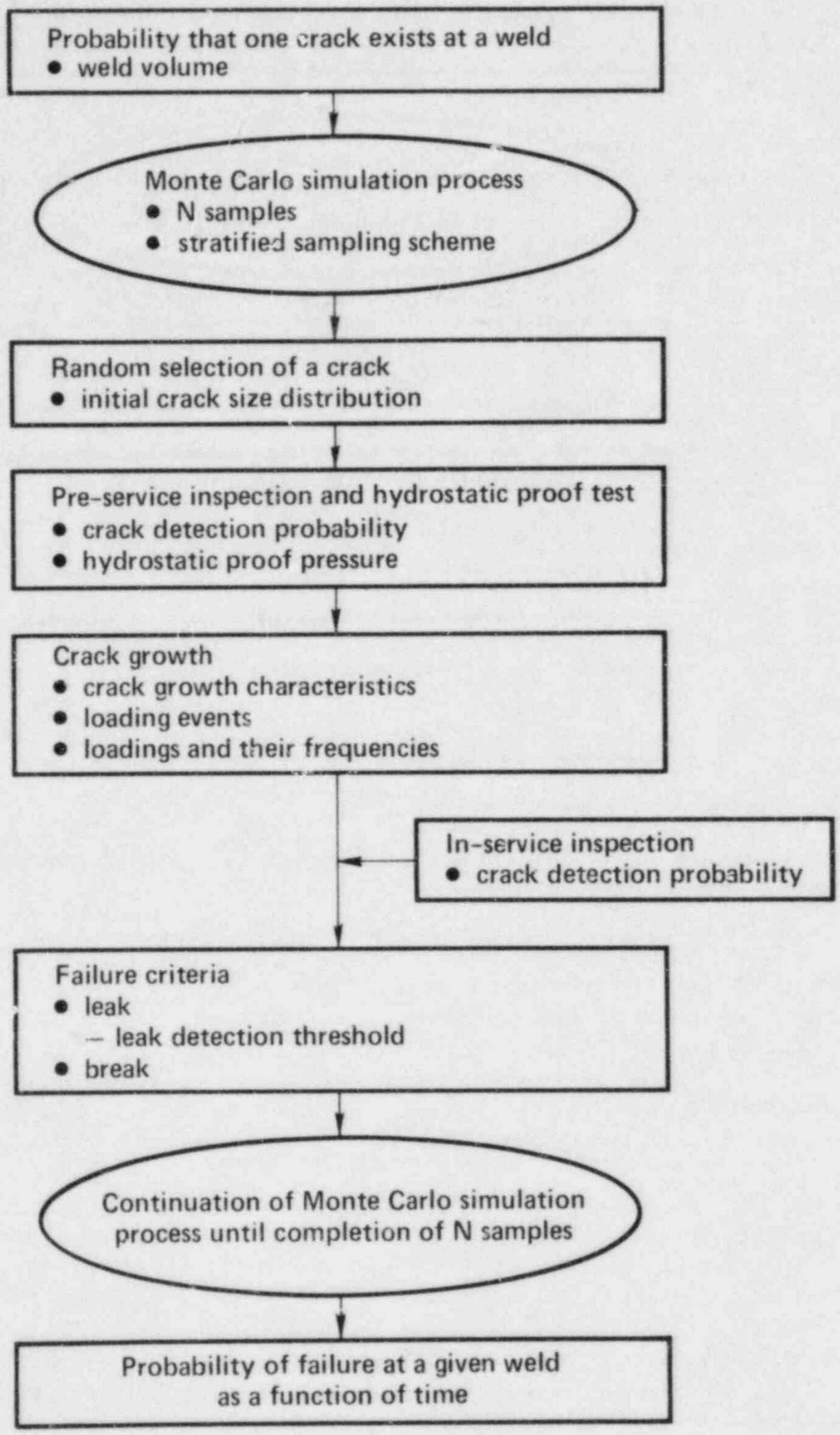

Figure 3. Computation flow chart for estimating the failure probability at a given weld.

failure at any weld in the loop. Assuming that each weld failure is an independent event, we can define the system piping failure by:

$$(P_f)_{sys} = 1 - \prod_{j=1}^{N} [1 - (P_f)_j] \quad , \tag{1}$$

where

$(P_f)_{sys}$ = the probability of failure in the RCL system piping,
$(P_f)_j$ = the probability that the jth joint in the system piping will fail,
N = the total number of weld joints in the system piping.

If we assume that the loops are identical, Eq. (1) becomes:

$$(P_f)_{sys} = 1 - \prod_{j=1}^{16} [1 - (P_f)_j]^L \quad , \tag{2}$$

where L represents the number of loops. This number varies from two to four for the RCL system piping in Westinghouse plants.

3.4 Uncertainties and Our Methods of Analysis

Many events affecting the RCL piping are rare and stochastic in nature (e.g., earthquakes), and estimating the probability of a failure due to them is a complex process. Simulation analysis is an appropriate method for this situation. Unfortunately, the assumptions and inputs for simulation analyses are usually subjective, resulting either from a lack of data or a lack of knowledge. Thus, the results of the analysis are uncertain.

There are three sources of variation associated with a simulation analysis:

(1) Random physical variation--This is inherent in the physical nature of the parameters. For example, the initial crack size in the RCL piping is not a single value, but is a distribution reflecting various causes resulting from different environments.

(2) Sampling process uncertainty--This is a random variation associated with the sampling process used in the simulation.

(3) Modeling uncertainty--This is the uncertainty associated with the models and inputs. This uncertainty considers variations in engineering judgments and expert opinions based on limited data for "true" models and inputs.

Since random physical variation is an inherent part of the physical world, it can not be eliminated by analysis. Its existence is the reason we are interested in finding a probability for the occurrence of pipe failures. The other sources of variations are associated with the analytical methods, and reflect our limited knowledge about certain parameters.

In the present analysis, the sampling uncertainty due to the stratified sampling process is expected to be small, so it is not considered in the analysis. We are therefore concerned with the other two uncertainties.

The input parameters with random physical variations are:

- Initial crack size: the initial crack depths and aspect ratios are considered to be random variables.
- Crack growth: fatigue crack growth is treated as being random.
- Flow stress: flow stress is treated as a random variable.

The input parameters considered as being subject to modeling uncertainty are:

- Initial crack depth distribution.
- Aspect ratio distribution in the initial cracks.
- Thermal expansion stresses.
- Seismic stresses.
- Seismic hazard curve.

The input parameters considered as being known without any uncertainty are:

- Volume of the weld material.
- Probability that a crack exists in the weld volume.
- Number of welds.
- Number of loops.
- Geometry of the pipe.
- Hydrostatic proof-test pressure.
- Dead weight stress.
- The pressure of the operating fluid.
- Design transient conditions.
- Leak detection threshold.

Considering the random physical variation in the piping reliability model along with the simulation process gives us a point estimate for the probability of a failure in the Westinghouse RCL piping. This point estimate is also known as the best estimate, because it uses the best available information for input parameters and models. The procedure for doing a best-estimate analysis is illustrated in Fig. 4.

An uncertainty analysis considers the uncertainties associated with the inputs and the models. It provides an estimate of the bounds, or limits, for the probability of a failure. We refer to these limits as "uncertainty bounds", and can also assign a measure of "confidence" to these estimates. Figure 5 shows the procedures used in doing an uncertainty analysis.

3.5 Important Events for the Analyses

It is desirable to express the results of the probability of failure analyses in terms of earthquake events, since earthquakes are of interest from both the design and safety evaluation standpoints. By assuming that earthquakes occur randomly over a given interval of time, the probability of n earthquakes occurring during the life of the plant can be expressed by the Poisson probability distribution:

$$P_n = (\lambda_o t)^n e^{-\lambda_o t}/n! \ , \quad n = 0,1,2,\ldots \ , \tag{3}$$

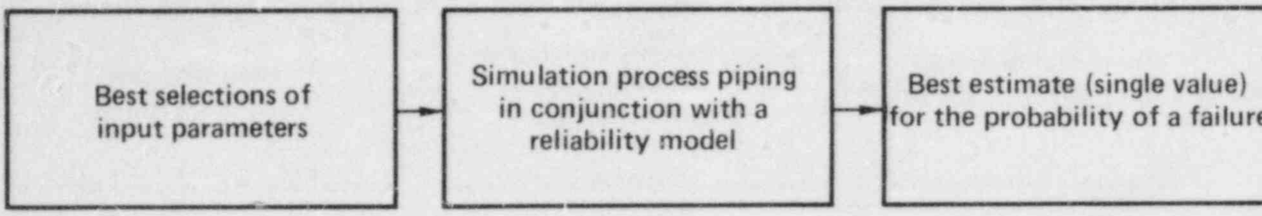

Figure 4. Procedures used in the best-estimate analysis.

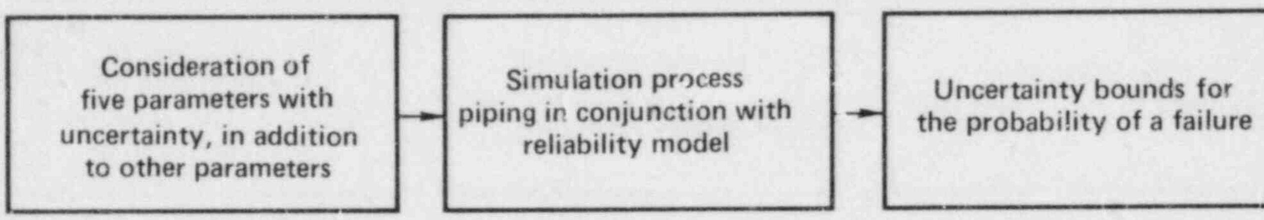

Figure 5. Procedures used in the uncertainty analysis.

where λ_o is the expected frequency of earthquakes per year, and t is the plant life.

Three scenarios related to an RCL piping failure during the plant's lifetime are of interest:

(1) An RCL piping failure occurs, but no earthquake occurs during the plant's lifetime.

(2) An RCL piping failure occurs before the first earthquake during the plant's lifetime.

(3) An RCL piping failure and the first earthquake during the plant's lifetime occur simultaneously.

The sum of the probabilities for these three scenarios gives the probability for the failure of the RCL piping during the plant's 40-year lifetime. The next three subsections list the formulas for calculating the probability for the occurrence of each scenario. (Details about the derivation of these formulas can be found in Reference 9.)

3.5.1 An RCL Piping Failure and No Earthquake

The probability for an RCL piping failure (under the no earthquake conditions) can be calculated by:

P(failure and no earthquake)

$$= \left\{ 1 - \prod_{j=1}^{16} [1 - P_j(F_j \mid \text{no earthquake})]^L \right\} e^{-40\lambda_o} \quad , \qquad (4)$$

where F_j represents the event that the jth weld fails during the life of the plant, and L is the number of loops in the RCL system.

3.5.2 An RCL Piping Failure Before the First Earthquake

The probability for an RCL piping failure before the first earthquake during the plant's lifetime can be calculated by:

P(failure before first earthquake)

$$= \int_0^{40} \{1 - \prod_{j=1}^{16} [1 - P_j(F_j \text{ prior to first earthquake} \mid T_f = t)]^L\}\lambda_o e^{-\lambda_o t}\, dt \quad (5)$$

where T_F is the time of the first earthquake.

3.5.3 Simultaneous RCL Piping Failure and First Earthquake

The probability of an RCL piping failure occurring simultaneously with the first earthquake can be calculated by:

P(failure and first earthquake)

$$= \int_{\hat{a}>\hat{a}} \int_0^{40} \{1 - \prod_{j=1}^{16} [1 - P_j(F_j \text{ at } t \mid T_F = t, \text{PGA} = \hat{a})]^L\} f(\hat{a})\lambda_o e^{-\lambda_o t}\, dt\, da \quad (6)$$

where $f(\hat{a})$, based on the seismic hazard curve, represents the frequency distribution of the peak ground acceleration (PGA), during an earthquake.

3.6 Interpretation of Results

The 17 sample plants are assumed to represent a random sample of the Westinghouse PWR plants east of the Rocky Mountains. To infer the empirical cumulative probability of a failure at any Westinghouse plant east of the Rocky Mountains from the sample plant analysis, we selected the graphical method shown in Fig. 6.

In this figure, the horizontal axis represents the probability of a failure; the vertical axis denotes the probability, ranging from 0 to 1, of not exceeding a particular probability of failure.

Given K samples, the values 1/K+1, 2/K+1, 3/K+1,..., K-1/K+1, K/K+1 on the vertical axis are plotted against the monotonically increasing probabilities for a failure, P_1, P_2,..., P_K, on the horizontal axis. A curve can then be drawn through these points to approximate the distribution of probabilities of failures for all the plants that are of interest. For example, in a best-estimate analysis, Fig. 6 provides the "best estimate" of the median probability for a failure, $P_{0.5}$. It also provides a best estimate for $P_{0.99}$, a value that is greater than the probabilities of failure at 99% of the Westinghouse plants.

This graphical method essentially estimates the probability of a failure in a large population, based on the results from a limited (but adequate) sampling. In Sections 4 and 5, we use this approach to estimate the probabilities for failures of the RCL piping, in the Westinghouse PWR plants east of the Rocky Mountains, by best-estimate and uncertainty analyses.

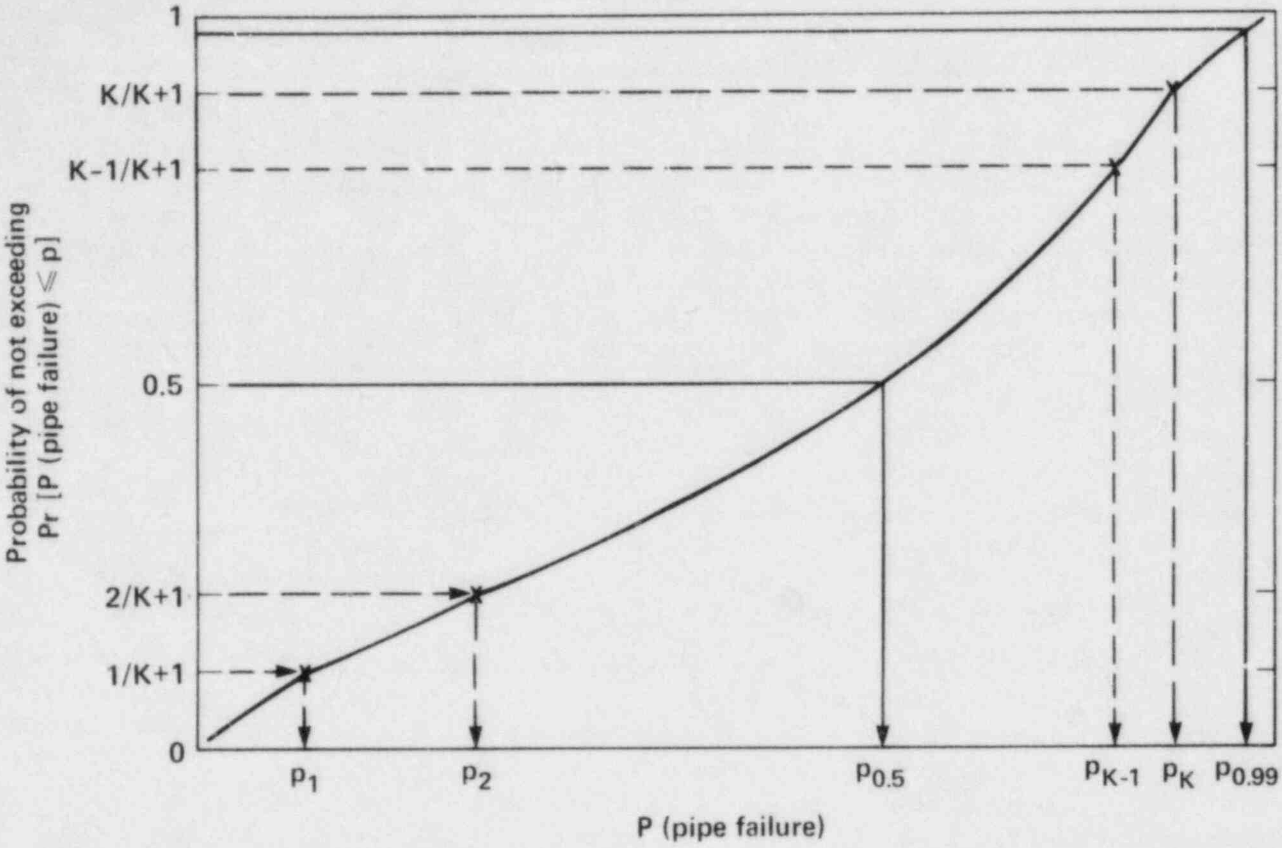

Figure 6. A graphical method used to derive the probability of failure in the RCL piping for large populations of Westinghouse PWR plants.

4. THE BEST ESTIMATE ANALYSIS

This analysis provides the best estimate for the probability of an RCL piping failure for each of the 17 Westinghouse sample plants east of the Rocky Mountains. Assuming that the 17 plants are a representative random sample of all the Westinghouse plants east of the Rocky Mountains, we further present a best estimate for the probability of an RCL piping failure for all of these plants. As previously mentioned, this uses the best estimates of the inputs to the piping reliability model.

4.1 Input Parameters for the Analysis

Following the computation flow chart for the piping reliability model of Fig. 3, we will first estimate the probability of a failure in each of the 16 circumferential girth butt weld joints in the RCL piping of each plant. We then estimate the probability of a failure in the RCL piping system as a whole, by combining the 16 probabilities. In the following subsections, we summarize the input parameters representing the best information for the analysis.

4.1.1 The Probability for the Existence of a Crack

If we assume that the cracks are created by the welding process, it is logical to relate the probability of a crack's existence to the weldment. If V denotes the weld volume, and λ_v is the rate of cracks per unit volume, and we assume a Poisson distribution for any cracks in V, the probability of having one crack, P_1, can be estimated by:[6]

$$P_1 = V\lambda_v \exp(-V\lambda_v) \quad . \tag{7}$$

Using a best estimate of λ_v as being equal to 0.0001 per cubic inch, and considering two pipe thicknesses, we have listed in Table 4 the probability for one crack existing in each RCL piping weld.

4.1.2 The Distribution of Initial Crack Size

Figure 7 shows an interior surface crack with a semi-elliptical shape, a crack depth of a, and a crack length of 2b.

Studies of the initial depth distribution of cracks, based on data from laboratories and from field experience, have been reported. A careful review of these studies led us to select Marshall's[10] model, in which a truncated exponential distribution represents the distribution of the initial crack depth, as given by the density function:

$$P_a(a) = \frac{e^{-a/\mu}}{\mu(1 - e^{-h/\mu})} \qquad 0 \le a \le h \quad , \tag{8}$$

where the best-estimate value of μ is 0.246 inch.

Table 4. Probability for the existence of one crack in eacn RCL piping weld.

Region of RCL	Weld joint number	Weld volume (cu in.)		P(existence of 1 crack)	
		Thickness A*	Thickness B*	Thickness A*	Thickness B*
Hot leg	1	1139	1276	0.1016	0.1274
	2	1139	1276	0.1016	0.1274
	3	2028	2554	0.1656	0.2077
	4	2028	2554	0.1656	0.2077
	5	2028	2554	0.1656	0.2077
Crossover leg	6	2137	2410	0.1726	0.2195
	7	1378	1554	0.1201	0.1528
	8	1378	1554	0.1201	0.1528
	9	1378	1554	0.1201	0.1528
	10	1378	1554	0.1201	0.1528
	11	2137	2410	0.1726	0.2195
Cold leg	12	2915	3307	0.2178	0.2803
	13	2915	3307	0.2178	0.2803
	14	978	1109	0.0887	0.1142
	15	978	1109	0.0087	0.1142
	16	1586	1799	0.1353	0.1741

*Refers to Table 2.

The aspect ratio, defined as $\beta = b/a$, is another parameter that describes crack size. The modified lognormal density distribution proposed by Harris[6] was selected to describe the aspect ratio distribution as follows:

$$P_\beta(\beta) = \begin{cases} 0, \text{ when } \beta < 1 \\ \dfrac{C_\beta}{\lambda\beta(2\pi)^{1/2}} \exp\left[-\left(\ln\dfrac{\beta}{\beta_m}\right)^2 / \left(2\lambda^2\right)\right], \text{ when } \beta > 1 \end{cases} , \tag{9}$$

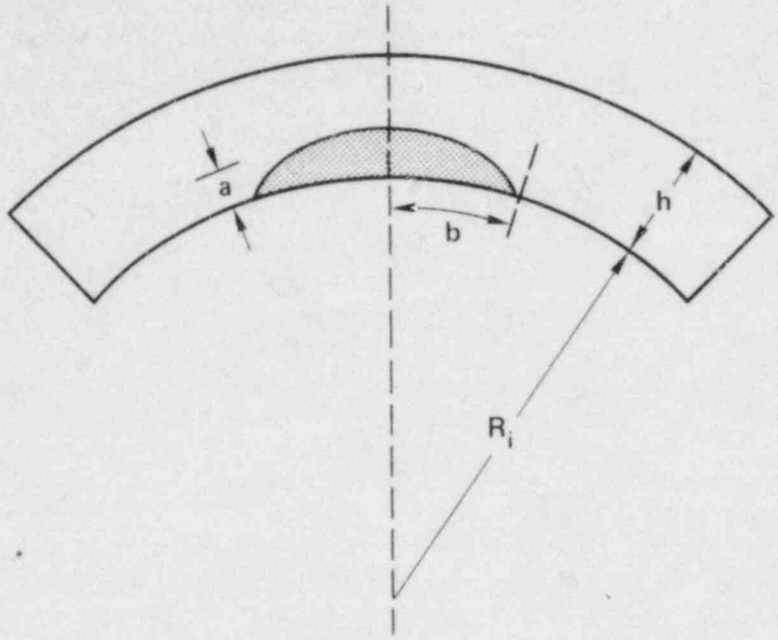

Figure 7. A circumferentially oriented semi-elliptical pipe crack with depth a, half-length b, inside radius R_i, and wall thickness h.

where $C_\beta = 1.419$, $\lambda = 0.5382$, and $\beta_m = 1.366$ (which correspond to a $P_\beta(\beta > 5) = 10^{-2}$) are the best estimate values used for the distribution.

4.1.3 The Probability of Detecting a Crack

Ultrasonic testing, a method of nondestructive examination, is often used for detecting cracks during preservice and inservice inspections. Only those cracks which escape detection by this method can grow any further. Therefore, we are interested in the probability of not detecting a crack, P_{ND}, which is a function of the crack's size, the material being tested, and the characteristics of the instrumentation. For cast austenitic steels, we have:[6]

$$P_{ND} = 0.5 \text{ erfc} \left(\nu \ln \frac{A}{A^*} \right)$$

$$A = \begin{cases} \dfrac{\pi a D_B}{4} , & \text{if } 2b < D_B \\ \dfrac{\pi ab}{2} , & \text{if } 2b > D_B , \end{cases} \tag{10}$$

where $\nu = 1.6$, erfc is a complementary error function, D_B (equal to 1 inch) is the ultrasonic beam diameter, and A^* (equal to $[h/2a]A$) is the area of a crack with an approximately 50% chance of being detected. Equation (10) indicates that the probability of not detecting a very small flaw is nearly 1, and the probability of not detecting a very large one is nearly 0.

4.1.4 Crack Growth Calculations

The structural material's subcritical crack-growth characteristics are an important input for the analysis. In the present instance, the material considered is basically Type 316 austenitic stainless steel, which has typically been used for the RCL piping at Westinghouse plants. This material has never been observed as being susceptible to stress corrosion cracking in the primary piping of PWRs. Attention was therefore concentrated on fatigue crack growth, with possible environmental influences being considered. Hence, corrosion fatigue is included in the analysis.

Crack growth caused by fatigue can be calculated by certain combinations of two variables; the range of the applied stress intensity factor, ΔK, and the load ratio, R. The load ratio is defined as K_{min}/K_{max}, with K_{min} and K_{max} representing the minimum and maximum stress intensity factors, respectively.

Using sufficient data on the fatigue crack growth rates of Types 304 and 316 stainless steels in a simulated PWR environment for a range of stress intensities, various load ratios, test frequencies, and specimen orientations, Harris proposed the following fatigue crack growth rate law:[6]

$$\frac{da}{dn} = \begin{cases} 0, \text{ when } \Delta\bar{K}_a < 4.6 \text{ ksi(in.)}^{1/2} \\ C\Delta\bar{K}_a^4 = C\left[\dfrac{\Delta K_a}{(1 - R)^{1/2}}\right]^4, \text{ when } \Delta\bar{K}_a > 4.6 \text{ ksi(in.)}^{1/2} \end{cases} \tag{11}$$

$$\frac{db}{dn} = \begin{cases} 0, \text{ when } \Delta\bar{K}_b < 4.6 \text{ ksi(in.)}^{1/2} \\ C\Delta\bar{K}_b^4 = C\left[\dfrac{\Delta K_b}{(1 - R)^{1/2}}\right]^4, \text{ when } \Delta\bar{K}_b > 4.6 \text{ ksi(in.)}^{1/2} \end{cases} \tag{12}$$

where n is the number of cyclic loads, C is a lognormal distribution (with a median equal to 9.4×10^{-12}, and a standard deviation of 2.2×10^{-11}), and ΔK_a and ΔK_b are the ranges of the applied stress intensity factors in the direction of the crack's depth and its length, respectively. (The unit, ksi, stands for kips/inch^2, where a kip equals a 1000 pound load.)

4.1.5 Loadings

Loadings considered in the fatigue-crack growth calculations consist of:

(1) The internal pressure in the pipe.

(2) The pipe's dead weight.

(3) The thermal expansion load on the pipe resulting from structural restraints.

(4) Seismic load.

(5) Transient thermal loads.

Appendix A contains information about the first four of these loadings. Transient conditions that lead to transient thermal loads are listed in Table 3.

For the transient thermal loads, the heatup and cooldown transients result in a uniform stress through the pipe wall's thickness, while other transients produce a thermal gradient stress across the pipe wall thickness. Section 4.2 compares the results obtained by considering only the heatup-cooldown transient condition with those obtained by considering all transient conditions.

For seismic loads, the intensity of an earthquake and the rate of occurrence for earthquakes with that intensity are important. The probabilities for seismic loads can be described by the seismic hazard curve (as described in Section 5.1.5). This curve shows the probability for the occurrence of at least one earthquake with a normalized peak acceleration, A = a/SSE, larger than the specified value. A mathematical model of the seismic hazard curve[11] used in the best-estimate analysis for plants east of the Rocky Mountains is:

$$P(A > a/SSE) = 2.9 \times 10^{-5}(a/SSE)^{-2.85} \quad , \qquad (13)$$

where SSE is the peak acceleration for a safe shutdown earthquake.

4.1.6 Failure Criteria

Failures are defined as being either by a leak or by a DEGB. Elastic-plastic failure criteria are required for a DEGB, since the austenitic piping steels are very tough and ductile. Basically, two types of elastic-plastic criteria can be used:

(1) Exceeding critical values for the J-integral and the tearing modulus.[12]

(2) Exceeding a critical net cross-sectional stress.

A study by Tada[12] shows that cracks will not become unstable in the type of reactor piping we are analyzing when the first criterion is applied. Therefore, we used the second criterion as the criterion for a DEGB.

Figure 8 shows the cross-section of a pipe with a circumferential crack, which is subjected to an external bending moment, M, and an axial force, N. The flawed pipe is at the point of incipient failure when the net section in the cracked plane forms a plastic hinge. An unrestrained plastic flow occurs at a critical stress level, σ_f, which is defined as being approximately equal to the average of the yield and the ultimate tensile strengths. The critical stress σ_f is usually called the flow stress.

The failure criterion, based on work by Kanninen et al.[13], is obtained by requiring that an equilibrium exist between the force and the moment of the cracked pipe. Assuming that the semi-elliptical crack area shown in Fig. 8 is

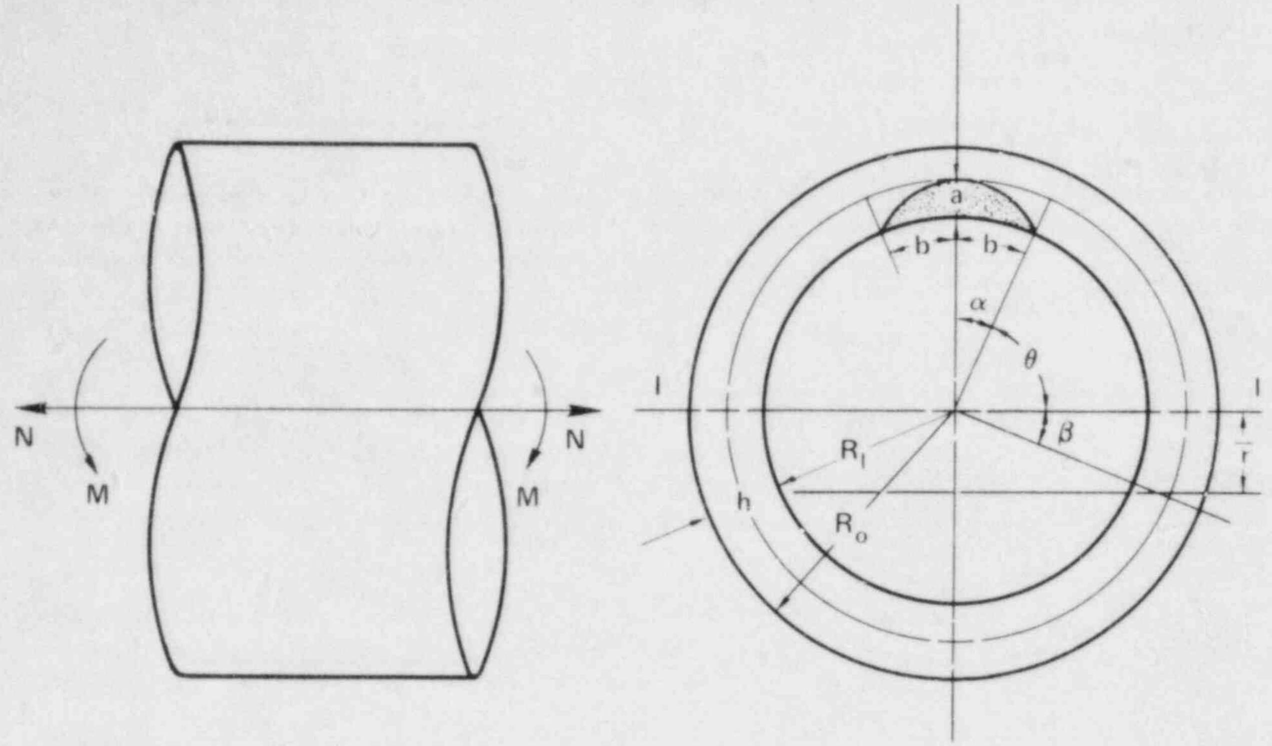

Figure 8. Cross section of a flawed pipe with a circumferential crack that is subjected to a bending moment and an axial force.

approximately equal to the hollow sector area, $2\alpha R_i a$, we can locate the new neutral axis of equilibrium, as follows:

$$|\bar{r}| = \frac{[(R_m)^2 h - (h - a)(R_m + [a/2])^2] \sin \alpha}{R_m h(\pi - \alpha) + \alpha(h - a)(R_m + [a/2])} \tag{14}$$

$$\beta = \sin^{-1}(\bar{r}/R_m) \quad , \tag{15}$$

where $R_m = (R_o + R_i)/2$ is the mean radius, and $\bar{r}$ is the distance from the original neutral axis (I-I line) to the new neutral axis. The critical moment and force, M_o and N_o, respectively, can then be related to the flow stress:

$$M_b = 2[(R_m)^2 \, h(2 \cos \beta - \sin \alpha) + (R_m + [a/2])^2(h - a) \sin \alpha]\sigma_f \quad , \tag{16}$$

$$N_o = 2(\pi - \alpha)R_m \, h\sigma_f + 2\alpha \, [R_i + (h + a)/2] \, (h - a) \, \sigma_f \quad . \tag{17}$$

For the reactor piping being considered here, we assumed that σ_f is normally distributed, with a mean value of 44.9 ksi and a standard deviation of 1.9 ksi.

A pipe instability leading to a DEGB is assumed when the following condition is satisfied:

$$\frac{M}{M_b} + \left(\frac{N}{N_o}\right)^2 \geq 1 \quad . \tag{18}$$

This criterion considers only load-controlled loads, which include the pipe's internal pressure, its dead weight, and the seismic load. Thermal loads are not included because they are classified as displacement-controlled loads, and contribute only to crack growth.

4.1.7 Other Inputs

A leak threshold of three gallons per minute was used in the analysis, reflecting the current practical instrumentation capability, as suggested by Westinghouse. Any coolant leakage above this threshold, resulting from a crack through the wall, is considered as detectable and would be repaired immediately.

Inservice inspections were not included in the analysis, since this program varies from plant to plant. The significance of our neglecting these inspections in this study is that we derive higher estimates for the failure probabilities.

The hydrostatic proof-test pressure is taken as having been 3.106 ksi for all weld-joint locations.

4.1.8 Numerical Simulation Method

Because of the complexities involved in treating many parameters as random variables, a Monte Carlo technique[14] is used to simulate the entire crack growth history for each weld joint. To increase the accuracy and computational efficiency of the Monte Carlo simulations, we used stratified sampling to select initial sizes for the simulated cracks. This sampling scheme is particularly powerful for assessing the rates of rare events (i.e., less than 10^{-6}) because only those crack samples that could lead to a leak or a DEGB are considered. Even using this powerful scheme, we still chose from 5000 to 6000 crack samples in the simulation process for each weld joint.

4.2 Results and Discussion

Best estimates for the probability of a failure in the RCL piping at each of the 17 sample plants are presented with respect to possible earthquake occurrences. During the lifetime of the plant, there are three possible scenarios with regard to an RCL piping failure and earthquakes (as described in Section 3.5):

(1) A pipe failure occurs without an earthquake during the plant's lifetime.

(2) A pipe failure occurs prior to the first earthquake during the plant's lifetime.

(3) A pipe failure and the first earthquake during the plant's lifetime occur simultaneously.

A test run, which considered all the design transients of the Model D steam generator (see Table 3), was first conducted to obtain a comparison with the results considering only heatup/cooldown transients. The comparison indicated that transient conditions other than heatup/cooldown conditions contributed very little (at most, 10%) to the results for the probability of a failure at each weld. This finding confirmed the conclusion reached in the Zion Unit 1 (steam generator Model 51) study. Therefore, all the results presented in this study are for the heatup/cooldown transients only.

Table 5 presents the best estimates of the cumulative probabilities for a leak occurring at the end of a 40-year plant life for the RCL piping at each of the 17 sample plants. It is interesting to note that the estimated leak probabilities for scenarios (1) and (2) are on the order of 10^{-6} to 10^{-7},

Table 5. Results of a best-estimate analysis for deriving cumulative probabilities for a leak, at the end of the 40-year plant life, for the RCL piping of the Westinghouse plants east of the Rocky Mountains.

	P(leak)			
Sample plant	No earthquake	Prior to 1st earthquake	Simultaneous with earthquake	Combined
1	2.4×10^{-7}	2.6×10^{-7}	6.5×10^{-12}	5.0×10^{-7}
2	2.1×10^{-6}	2.4×10^{-6}	3.4×10^{-10}	4.5×10^{-6}
3	4.5×10^{-7}	4.9×10^{-7}	5.5×10^{-11}	9.4×10^{-7}
4	1.9×10^{-6}	2.0×10^{-6}	2.6×10^{-10}	3.9×10^{-6}
5	2.9×10^{-6}	3.1×10^{-6}	3.1×10^{-10}	6.0×10^{-6}
6	2.1×10^{-6}	2.3×10^{-6}	6.3×10^{-10}	4.4×10^{-6}
7	2.5×10^{-6}	2.7×10^{-6}	5.1×10^{-11}	5.2×10^{-6}
8	2.1×10^{-6}	2.2×10^{-6}	8.6×10^{-10}	4.3×10^{-6}
9	1.0×10^{-6}	1.1×10^{-6}	3.7×10^{-11}	2.1×10^{-6}
10	3.5×10^{-7}	3.7×10^{-7}	9.8×10^{-12}	7.2×10^{-7}
11	2.7×10^{-6}	2.9×10^{-6}	2.4×10^{-10}	5.6×10^{-6}
12	1.4×10^{-6}	1.5×10^{-6}	2.8×10^{-11}	2.9×10^{-6}
13	1.6×10^{-6}	1.7×10^{-6}	1.8×10^{-10}	3.3×10^{-6}
14	2.3×10^{-6}	2.4×10^{-6}	1.4×10^{-9}	4.7×10^{-6}
15	1.8×10^{-6}	1.9×10^{-6}	7.0×10^{-11}	3.7×10^{-6}
16	2.9×10^{-6}	3.1×10^{-6}	6.7×10^{-10}	6.0×10^{-6}
17	1.3×10^{-6}	1.4×10^{-6}	1.9×10^{-10}	2.7×10^{-6}

that the leak probability for event (3) is several orders of magnitude lower; on the order of 10^{-9} to 10^{-12}. This implies that the simultaneous occurrence of a pipe leak and the first earthquake is much less likely than a pipe leak with no earthquakes during the plant's lifetime, or a pipe leak prior to the first earthquake. Therefore, the estimated cumulative probability for leaks due to all three scenarios is approximately equal to the estimated cumulative probability for only scenarios one and two. The estimated cumulative probability for a leak at the end of a 40-year plant life, for the RCL piping in our sample plants, ranges from 5.0×10^{-7} to 6.0×10^{-6}.

It is a common practice to express a probability of failure as a rate per plant year, even though the probabilities vary from year to year. We neglected such variations, and approximated the probability of a leak per plant year by averaging the cumulative probability that a leak will occur at the end of plant's life. Figure 9 shows an empirical cumulative distribution for the probability of a leak per plant year for the sample plants. The 99th-percentile, $P_{0.99}$, for the probability of a leak in the RCL (using a best-estimate analysis) is thus estimated as being 1.6×10^{-7} per plant year for all Westinghouse plants east of the Rocky Mountains. In other words, it can be inferred that 99% of the Westinghouse PWR plants east of the Rocky Mountains have a probability, that an RCL piping leak will occur, of less than 1.6×10^{-7} per plant year.

Table 6 presents, for the RCL piping at each sample plant, the cumulative probabilities that a DEGB will have occurred at the end of the 40-year plant life. We found that the DEGB probabilities for the three scenarios involving earthquake roles resembled those found for the leak probabilities. The cumulative probability that a DEGB will occur for the first and second scenarios is 10^{-10} to 10^{-11}, whereas the probability that the third scenario will happen ranges from 10^{-12} to 10^{-15}. It appears that if a DEGB failure occurs in the RCL piping, it will result from loadings other than those caused by earthquakes. For example, the contribution from earthquakes at sample plant 14 to the probability of a DEGB in the RCL piping is merely 0.84% of the contribution from other loadings.

This sheds some light on the role that earthquakes play in DEGB failure in the RCL piping. Most importantly, we found that the cumulative probabilities for a DEGB from all three scenarios at our sample plants are on the order of 10^{-10} to 10^{-11}, which are extremely low values. From the probabilistic point of view, this simply says that a DEGB failure in the RCL piping is a very unlikely event.

The cumulative DEGB probability can also be expressed in terms of an average DEGB probability per plant year. Figure 10 shows the empirical cumulative distribution for the probability of a DEGB per plant year for the sample plants. Following the procedure described earlier, for all Westinghouse plants east of the Rocky Mountains, we estimate that the 99th-percentile, $P_{0.99}$, for the probability of an RCL piping DEGB (using a best-estimate analysis) is 6.8×10^{-12} per plant year. Or, it can be stated that 99% of the Westinghouse PWR plants east of the Rocky Mountains have a probability for a DEGB failure in the RCL piping of less than 6.8×10^{-12} per plant year.

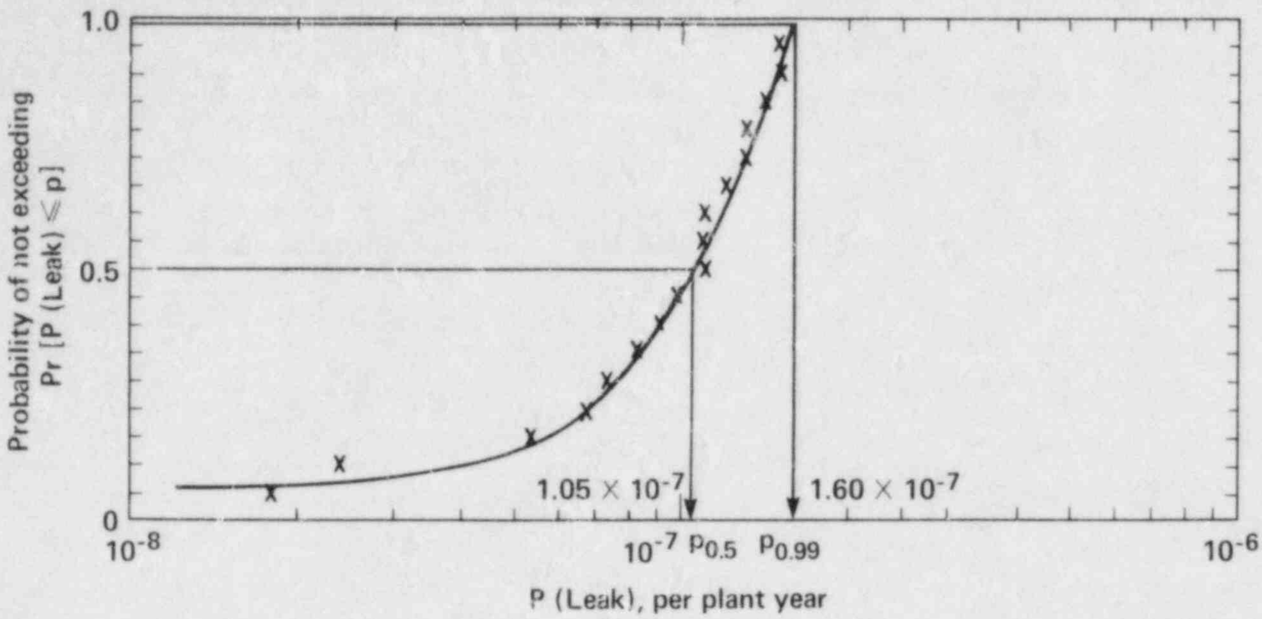

Figure 9. Empirical cumulative distributions for the probability of leaks in Westinghouse PWR plants east of the Rocky Mountains.

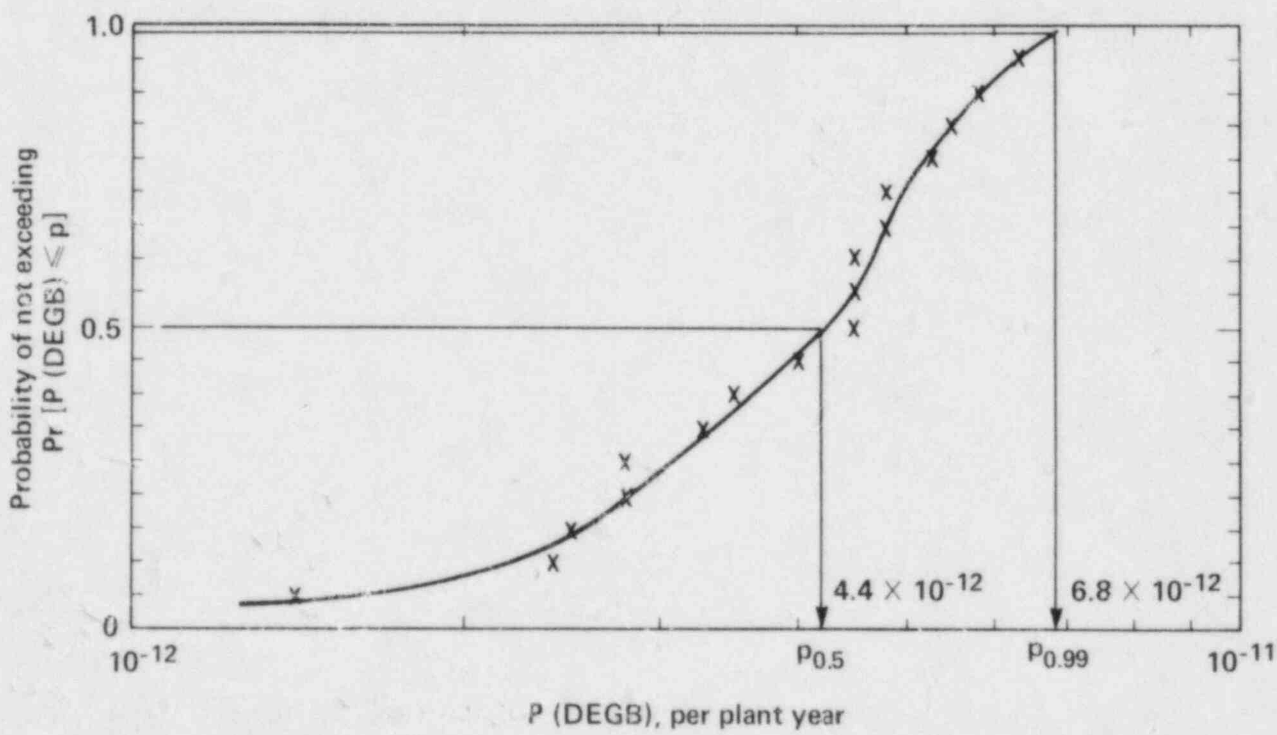

Figure 10. Empirical cumulative distributions of the probability for a double-ended guillotine break (DEGB) in Westinghouse PWR plants east of the Rocky Mountains.

Table 6. Results of a best-estimate analysis for deriving cumulative probabilities for a DEGB, at the end of the 40-year plant life, for the RCL piping in the Westinghouse plants east of the Rocky Mountains.

	P(DEGB)			
Sample plant	No earthquake	Prior to 1st earthquake	Simultaneous with earthquake	Combined
1	1.6×10^{-11}	2.8×10^{-11}	7.6×10^{-15}	4.4×10^{-11}
2	8.6×10^{-11}	9.3×10^{-11}	3.0×10^{-13}	1.8×10^{-10}
3	5.0×10^{-11}	5.4×10^{-11}	7.4×10^{-14}	1.0×10^{-10}
4	9.4×10^{-11}	1.0×10^{-10}	4.7×10^{-13}	1.9×10^{-10}
5	7.8×10^{-11}	8.4×10^{-11}	1.2×10^{-13}	1.6×10^{-10}
6	8.7×10^{-11}	9.4×10^{-11}	1.1×10^{-12}	1.8×10^{-10}
7	1.1×10^{-10}	1.2×10^{-10}	1.6×10^{-14}	2.3×10^{-10}
8	1.0×10^{-10}	1.1×10^{-10}	1.4×10^{-12}	2.1×10^{-10}
9	4.7×10^{-11}	5.0×10^{-11}	2.1×10^{-14}	9.7×10^{-11}
10	5.2×10^{-11}	5.6×10^{-11}	4.1×10^{-14}	1.1×10^{-10}
11	9.3×10^{-11}	1.0×10^{-10}	8.8×10^{-14}	1.9×10^{-10}
12	1.1×10^{-10}	1.1×10^{-10}	2.4×10^{-13}	2.2×10^{-10}
13	5.5×10^{-11}	5.9×10^{-11}	1.2×10^{-13}	1.1×10^{-10}
14	1.2×10^{-10}	1.3×10^{-10}	2.1×10^{-12}	2.5×10^{-10}
15	6.9×10^{-11}	7.5×10^{-11}	1.8×10^{-14}	1.4×10^{-10}
16	8.8×10^{-11}	9.4×10^{-11}	4.9×10^{-13}	1.8×10^{-10}
17	6.1×10^{-11}	6.5×10^{-11}	1.5×10^{-13}	1.3×10^{-10}

5. THE UNCERTAINTY ANALYSIS

Our uncertainty analysis estimates the bounds or limits reflecting the uncertainties in the failure probability calculations, due to some of the input parameters being based on limited data, or on individual judgments, rather than on their being precisely known. This type of uncertainty is usually referred to as modeling uncertainty. From a sensitivity study,[6] and a review of all the input parameters, we decided to focus on five parameters in the uncertainty analysis.

In the following sections we discuss the details of these parameters, describe how the simulation process was carried out with uncertain parameters, and then present our results and a discussion of the uncertainty analysis.

5.1 Parameters That Have Modeling Uncertainties

Five parameters have significant modeling uncertainties: the initial depth distribution of cracks, the initial distribution for the aspect-ratios of the cracks, the thermal expansion loads, the seismic load, and the seismic hazard curve.

5.1.1 The Depth Distribution of Initial Cracks

Figure 11 shows various complementary cumulative distributions for the depths of the initial cracks. Among these, the Marshall distribution falls within the estimates made by Lynn,[15] and is generally within an order of magnitude of Becher's and Hansen's lognormal fit.[16] The Wilson[17] distribution $b_o > 2$ inches falls well below all the others. This is at least partly due to its exclusion of cracks with initial half-surface lengths of less than two inches. This led us to place emphasis on Marshall's, rather than Wilson's distribution. An exponential function that describes the Marshall distribution shown in Fig. 11 is:

$$P_a\ (> a) = \exp\ (-a/\mu)\ , \tag{19}$$

where $\mu = 0.246$ inch is the mean crack depth.

Using Marshall's model for the distribution of crack depths, we selected an upper bound with $\mu = 0.33$ inch, to cover all the distributions we have discussed.[15,16] For the lower bound, we took a conservative approach and selected $\mu = 0.2$ inch to discount distributions such as those of Wilson, and of Becher and Hansen. We believe that these uncertainty bounds represent a reasonable agreement between Marshall's findings and Lynn's estimates. After defining these uncertainty bounds, we also assumed that the reciprocal of μ, $\alpha = 1/\mu$, is a triangular random variable with a range of from 3 to 5 inch^{-1}.

Some modifications were made to Eq. (19) to eliminate the physical impossibility of having a crack depth that exceeds the thickness of the pipe's wall. This was accomplished by renormalizing the density function, $P_a\ (a) = \exp\ (-a/\mu)/\mu_1$, which leads to the following complementary cumulative distribution of crack depth:[6]

$$P_a(> a) = \frac{\exp(-a/\mu) - \exp(-h/\mu)}{1 - \exp(-h/\mu)}\ . \tag{20}$$

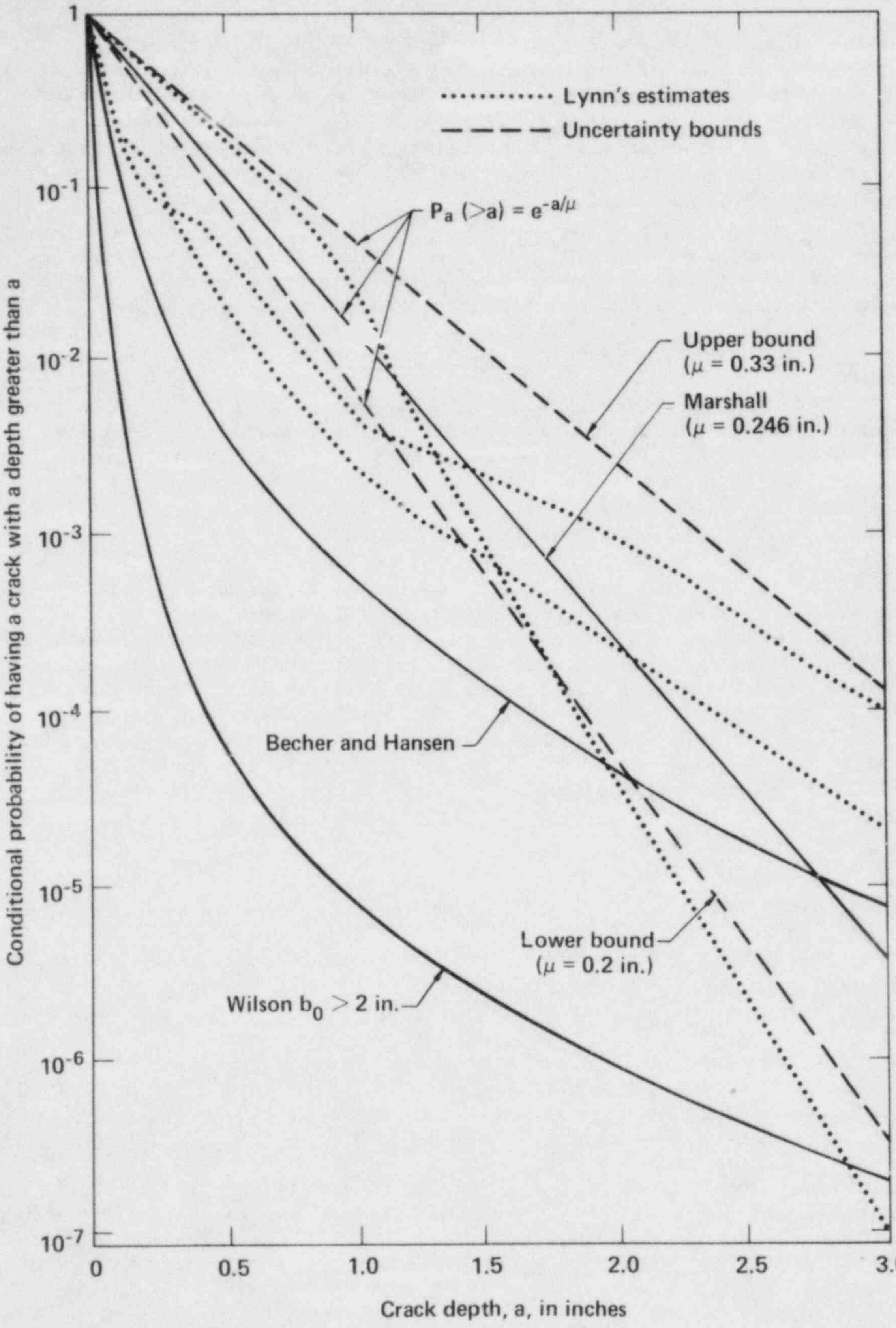

Figure 11. Various distributions and selected uncertainty bounds for the cumulative marginal distributions of initial crack depths.

5.1.2 The Aspect-Ratio Distribution of Initial Cracks

Information about the aspect-ratic distribution for initial cracks is scarce. Based on our field experience, cracks seldom have an aspect ratio less than that for a semicircle ($\beta = 1$). We therefore assumed that a truncated lognormal function ($\beta > 1$) could be used for the aspect-ratio distribution of the initial cracks. This distribution has the following form:[6]

$$P_\beta(\beta) = \begin{cases} 0, \text{ when } \beta < 1 \\ \dfrac{C_\beta}{\lambda\beta(2\pi)^{1/2}} \exp\left[-\left(\ln \dfrac{\beta}{\beta_m}\right)^2 \Big/ \left(2\lambda^2\right)\right], \text{ when } \beta > 1 \end{cases} \tag{21}$$

where C_β, λ, and β_m are parameters of the distribution function. They can be determined by:

$$\int_1^\infty P_\beta(x)dx = 1 \tag{22}$$

$$\int_5^\infty P_\beta(x)dx = \rho \tag{23}$$

$$\beta_m \exp(-\lambda^2) = 1 \quad . \tag{24}$$

Equation (24) defines the mode of the lognormal distribution at $\beta = 1$. Physically, ρ is that fraction of the crack population with an aspect ratio β greater than five.

The uncertainty analysis associated with this distribution was done by treating the median of the cracks' aspect ratios, β_m, as a lognormal random variable with a median of 0.29 and a coefficient of variation equal to 0.086, derived from the input: $\beta_m = 1.336$ and 1.158 for the 50th and 5th percentiles, respectively. Figure 12 shows three cumulative marginal distribution curves, corresponding to the 99.9th- ($\rho = 10^{-1}$), 50th- ($\rho = 10^{-2}$), and 5th- ($\rho = 10^{-4}$) percentiles for the distribution of the β_m values 1.736, 1.336, and 1.158, respectively. (Note that the 50th-percentile curve [$\beta_m = 1.336$, $\lambda = 0.5382$, $C_\beta = 1.419$] was used for the aspect-ratio distribution of initial cracks in the best-estimate analysis of Section 4.)

5.1.3 Thermal Expansion Loads

The calculation of loads resulting from thermal expansion is straightforward. However, it was judged that the design thermal expansion loads are usually greater than the true values. We did not, however, rule out the possibility that the converse could be true. Therefore, we assumed that the thermal expansion load is a lognormal random variable to reflect its uncertainty under two conditions:

(1) The median value is 80% of the design load.

(2) There is only a 10% probability that the true thermal expansion load exceeds the calculated load.

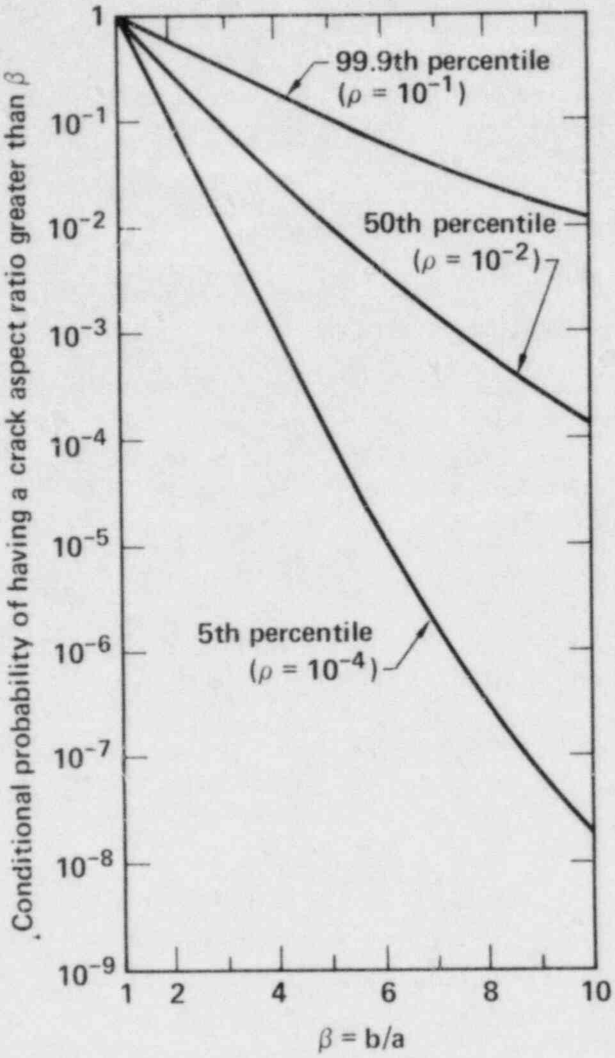

Figure 12. Uncertainty bounds for the cumulative marginal distributions of crack aspect ratios.

These conditions yield a value of 0.1547 for the coefficient of variation. (Note that, in our best-estimate analysis in Section 4, the thermal expansion loads at each weld joint were treated as being constant and equal to the median value.)

5.1.4 Seismic Loads

The calculation of seismic loads involves free-field ground motion, soil-structure interaction, and in-structure response. Because of the calculational complexities, simplified methods of analysis (which incorporate conservative assumptions) are used for design purposes. In the probabilistic approach, however, realistic inputs are desirable so that the result will reflect reality.

In the data package provided by Westinghouse, a design analysis approach was used to derive the seismic design loads. Ideally, these data and the assumptions used in the analyses should be studied on a plant-by-plant basis. Specific factors of conservatism for each plant would then be identified and applied to the seismic design loads to obtain the real seismic loads. This approach was not possible for us because of a lack of detailed data and time constraints. Instead, we chose one plant (Zion Unit 1) for which detailed information is available, for the comparison between design load and realistic load.

One common aspect of the seismic data package for most plants is that response-spectrum methods were used in the design analyses. We tried to estimate the degree of conservatism involved in the response-spectrum method. Two studies were conducted to identify the conservatism factor at Zion Unit 1.

In the first study, thirty multiply-supported time-history analyses were performed. The Seismic Methodology Analysis Chain with Statistics (SMACS) methodology, developed for the Seismic Safety Margins Research Program (SSMRP), was used.[18] The input for each time history analysis was a set of three synthetic ground acceleration records with their spectra enveloping the design spectra given in Regulatory Guide 1.60.[19] The response of the RCL piping was obtained by taking the median value of the responses from the 30 analyses.

In the second study, we used the response-spectrum analysis method.[20,21] From the 30 seismic time-history records used in the first study, we selected three at random. From these time histories, we generated three sets of response spectra at the RCL piping support locations. The procedure followed for combining and smoothing the floor-response spectra (with peaks broadened ±15%) was in accordance with Regulatory Guide 1.122,[22] to obtain the floor design-response spectra at those support locations. Applying each of three sets of design-response spectra to the RCL piping supports gave the corresponding RCL piping responses. Their average response was taken as the result of our response spectrum analysis.

Stress results for both the response-spectrum and time-history analyses are shown in Fig. 13 for each weld joint in the Zion Unit 1 4-loop RCL piping. Comparing the two analytical methods indicates that the response-spectrum analysis is the more conservative. The conservatism factor was defined as the ratio of the response-spectrum stress results to the time-history stress results, and was calculated for each weld joint and loop. By assuming a lognormal distribution for these factors, so as to reflect their uncertainties, we obtained a median value of 7.76 and a coefficient of variation of 0.362. The distribution of the conservatism factors for the seismic design loads in the Zion Unit 1 study was assumed to be applicable to the RCL piping of other plants. We did this to reduce the conservatism incorporated in the design practice. (Note that the median value for the conservatism factor was used to convert the design seismic load to the realistic load in our best-estimate analysis of Section 4.)

5.1.5 Generic Seismic Hazard Curves

Since the seismic hazard curve gives an annual probability for the occurrence of earthquakes with various peak ground accelerations, the curve is site dependent. For a given site, the curve is derived by combining recorded data, the estimated magnitudes of historic seismic events, a review of local geological studies, and opinion surveys of seismologists and geologists familiar with the region.

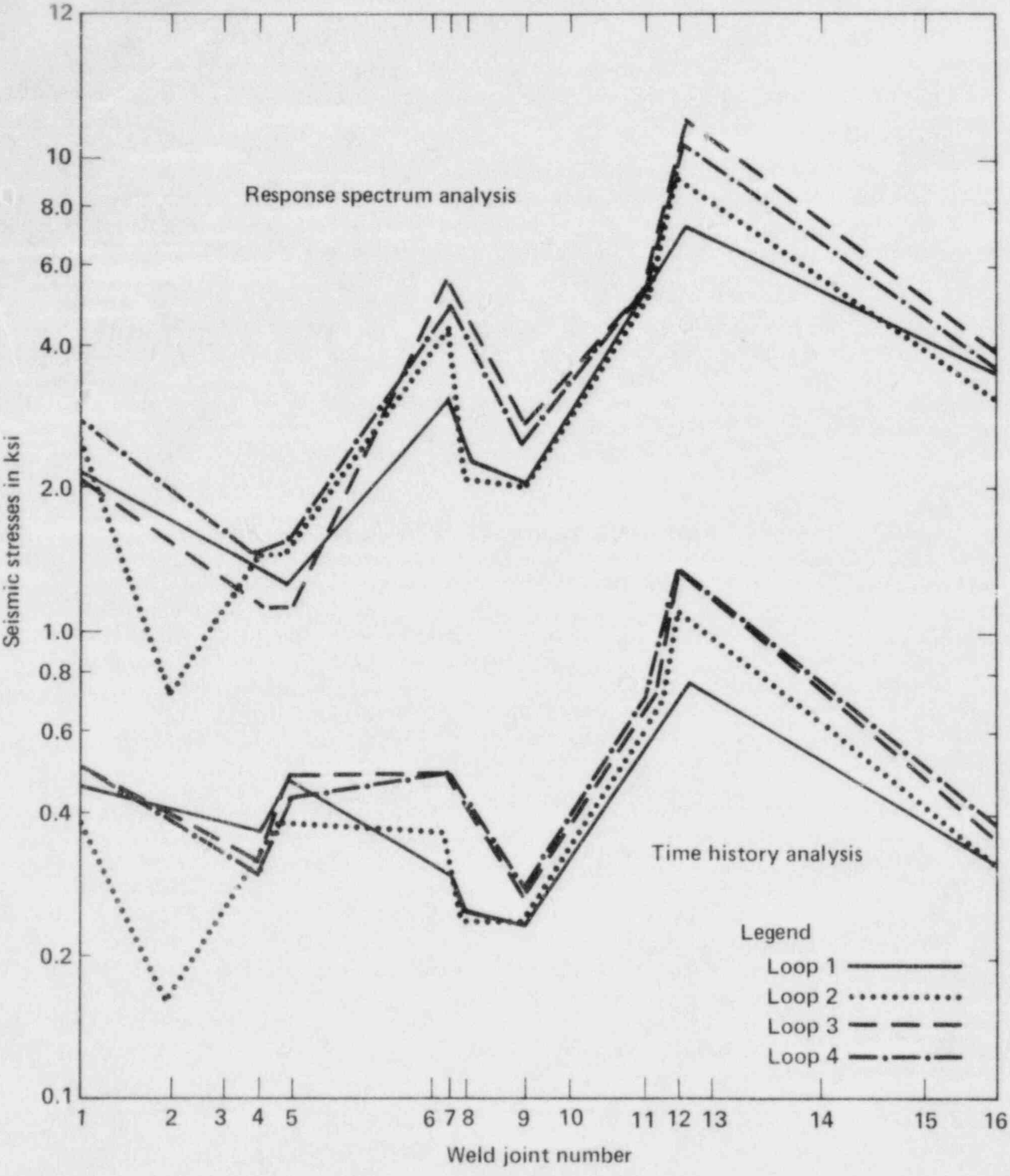

Figure 13. A comparison of seismic stresses between the response-spectrum and time-history analyses for weld joints in the RCL piping of the Zion Unit 1 plant.

In our study, however, the site-specific seismic hazard information for all the sample plants is not available. To be practical, we used the generic seismic curves to represent all of the plant sites east of the Rocky Mountains. The procedures used in deriving the curves are given in Vol. 4 of this report series.[10] Figure 14 shows a median generic seismic hazard curve, and the corresponding 90th- and 10th-percentile curves. The peak ground acceleration, a, was normalized with respect to the acceleration of a safe shutdown earthquake (SSE).

To account for the uncertainty associated with the generic seismic hazard curves, we first assumed that these curves can be mathematically expressed by:

$$P(A > a/SSE) = \alpha (a/SSE)^{-\beta} \quad , \tag{25}$$

where $P(A > a/SSE)$ represents the annual probability of having an earthquake with an intensity, A, larger than a/SSE, and where α and β are parameters used for curve fitting.

The values of $P(A > a/SSE)$ at values of a equal to 0.6 and 4 SSE were treated as lognormal random variables. Using the 10th-, 50th-, and 90th-percentile curves shown in Fig. 14, we obtained the parameters required for defining the lognormal distribution at a = 0.6 SSE and 4 SSE, as presented in Table 7.

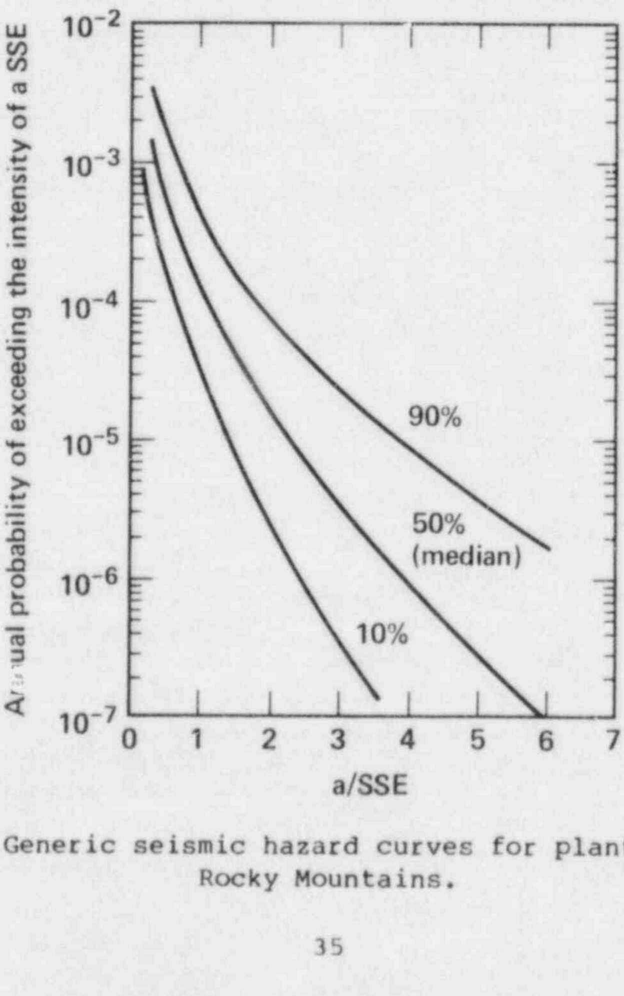

Figure 14. Generic seismic hazard curves for plants east of the Rocky Mountains.

Table 7. Parameters for describing the distribution of P(A > a/SSE).

Parameter	a = 0.6 SSE	a = 4 SSE
Median of P	1.5×10^{-4}	9.4×10^{-7}
Standard deviation for ln P	1.013	1.838

With P values randomly selected at a = 0.6 SSE and 4 SSE, we determined the associated parameters, α and β, used in Eq. (25). By using this method, we formulated a family of generic seismic hazard curves for the uncertainty analysis. (Note that we used the 50th-percentile curve in Fig. 14 as the seismic hazard input for our best-estimate analysis.)

5.2 Selecting Samples for the Uncertainty Analysis

In Section 5.1, we described the distributions of five parameters having uncertainties. This section describes how to create the samples by selecting these parameters from their distributions for the uncertainty analysis. We used a Latin hypercube sampling technique, with the following basic procedures:[20]

(1) Divide each random parameter into N equal-probability intervals.

(2) For each random parameter, randomly select a value within each interval.

(3) Arrange N combinations of five parameters with uncertainties. For each combination, an interval was randomly selected, without replacement, from the N equal-probability intervals for each parameter.

The N combinations are a sample of N equal-probability points in the 5-dimensional space of values for the uncertain parameters. In our study, we chose N as equal to 17 (an arbitrary value which, by coincidence, also equals the number of sample plants).

Ideally, this sampling technique should be applied to assess the uncertainty bounds of failure probability for each sample plant. An examination of the DEGB probability results (Table 6) obtained by the best-estimate analysis reveals that the DEGB probabilities lie in a narrow range (from 10^{-10} to 10^{-11}). This finding hints that the uncertainty bounds may have similar characteristics for all the sample plants. This conjecture was verified by conducting two uncertainty analyses, (for the plants having the lowest and the highest DEGB probabilities, respectively, as defined by the best-estimate analysis results). In other words, any sample plant can be used as a representative plant for estimating the relative uncertainty bounds for the DEGB probabilities at the other sample plants. We selected the representative plant with the highest probability estimate for the occurrence of a DEGB (sample plant 14), as determined by the best-estimate analysis. In Section 5.3, we present the uncertainty analysis results for this plant. These results are then extended to estimate the uncertainty bounds for the

Table 8. Results of the uncertainty analysis for deriving cumulative probabilities of a leak, at the end of the 40-year plant life, in the RCL piping of the sample plant with the highest probability for a DEGB.

	P(leak)			
Sample point[a]	No earthquake	Prior to 1st earthquake	Simultaneous with earthquake	Combined
1	4.4×10^{-7}	4.0×10^{-6}	5.8×10^{-8}	4.5×10^{-6}
2	1.2×10^{-7}	3.8×10^{-7}	5.4×10^{-10}	5.0×10^{-7}
3	8.7×10^{-6}	1.6×10^{-5}	2.5×10^{-8}	2.5×10^{-5}
4	3.4×10^{-7}	2.8×10^{-6}	1.4×10^{-8}	3.1×10^{-6}
5	8.2×10^{-8}	9.7×10^{-7}	5.5×10^{-9}	1.1×10^{-6}
6	2.8×10^{-7}	1.4×10^{-6}	7.1×10^{-9}	1.7×10^{-6}
7	6.5×10^{-7}	8.2×10^{-7}	5.0×10^{-10}	1.5×10^{-6}
8	7.3×10^{-7}	1.8×10^{-6}	4.1×10^{-9}	2.5×10^{-6}
9	3.6×10^{-13}	4.3×10^{-7}	2.3×10^{-8}	4.5×10^{-7}
10	2.8×10^{-9}	2.0×10^{-6}	1.4×10^{-8}	2.0×10^{-6}
11	4.1×10^{-7}	2.3×10^{-6}	7.3×10^{-9}	2.7×10^{-6}
12	1.2×10^{-8}	1.1×10^{-6}	1.4×10^{-8}	1.1×10^{-6}
13	1.7×10^{-7}	1.1×10^{-6}	6.2×10^{-9}	1.3×10^{-6}
14	1.4×10^{-6}	4.1×10^{-6}	9.8×10^{-9}	5.5×10^{-6}
15	1.6×10^{-6}	8.0×10^{-6}	7.9×10^{-8}	9.7×10^{-6}
16	1.9×10^{-13}	5.1×10^{-6}	3.6×10^{-8}	5.1×10^{-6}
17	1.1×10^{-6}	3.2×10^{-6}	9.8×10^{-9}	4.3×10^{-6}

[a] Refers to the sample number, as designated in the Latin hypercube sampling technique.

probability of a failure in the RCL piping for all of the Westinghouse plants east of the Rocky Mountains.

5.3 Results and Discussion

Using the criteria just outlined, sample plant 14 was selected (see Table 6). Table 8 presents the results for the cumulative probability (calculated by using the 17 sample points of plant 14's uncertainty analysis) that a leak will occur at the end of the plant's 40-year life. Note that the spread of the combined cumulative leak probabilities is very narrow, ranging from 10^{-5} to 10^{-7}. This implies that the leak probability estimates are not sensitive to the uncertainty bounds of the five parameters.

Table 9. Results of the uncertainty analysis for deriving cumulative probabilities for a DEGB, at the end of the 40-year plant life, for the RCL piping of the sample plant with the highest probability for a DEGB.

	P(DEGB)			
Sample point[a]	No earthquake	Prior to 1st earthquake	Simultaneous with earthquake	Combined
1	4.8×10^{-11}	4.8×10^{-10}	1.7×10^{-10}	7.0×10^{-10}
2	1.6×10^{-14}	5.8×10^{-14}	9.9×10^{-16}	7.5×10^{-14}
3	2.0×10^{-10}	3.8×10^{-10}	7.4×10^{-12}	5.9×10^{-10}
4	4.6×10^{-15}	3.5×10^{-14}	5.9×10^{-15}	4.5×10^{-14}
5	8.2×10^{-11}	1.1×10^{-9}	1.1×10^{-10}	1.3×10^{-9}
6	2.7×10^{-12}	1.5×10^{-11}	1.5×10^{-12}	1.9×10^{-11}
7	4.3×10^{-10}	5.6×10^{-10}	9.8×10^{-12}	1.0×10^{-9}
8	1.9×10^{-12}	5.0×10^{-12}	5.0×10^{-13}	7.4×10^{-12}
9	1.6×10^{-18}	2.7×10^{-11}	7.7×10^{-14}	2.7×10^{-11}
10	2.5×10^{-19}	2.9×10^{-16}	1.2×10^{-17}	3.0×10^{-16}
11	1.0×10^{-9}	6.6×10^{-9}	3.9×10^{-10}	8.0×10^{-9}
12	7.6×10^{-13}	8.0×10^{-11}	9.2×10^{-12}	1.4×10^{-10}
13	1.2×10^{-9}	9.2×10^{-9}	8.1×10^{-10}	1.1×10^{-8}
14	4.7×10^{-10}	1.5×10^{-9}	6.9×10^{-11}	2.0×10^{-9}
15	9.9×10^{-13}	5.7×10^{-12}	2.2×10^{-12}	8.9×10^{-12}
16	2.2×10^{-17}	9.4×10^{-10}	1.7×10^{-10}	1.1×10^{-9}
17	1.5×10^{-10}	5.2×10^{-10}	3.1×10^{-11}	7.0×10^{-10}

[a] Refers to the sample number, as designated in the Latin hypercube sampling technique.

Table 9 presents the cumulative probability that a DEGB will occur at sample plant 14. The combined cumulative DEGB probabilities at the end of the 40-year plant life show wide variations, from 10^{-8} to 10^{-16}, among the 17 sample points. This finding reveals that the uncertain parameters are more sensitive to the probability that a DEGB will occur than they are to the probability that a leak will occur.

The average probability for a failure per plant-year can be obtained by averaging the cumulative probabilities for a failure at the end of the plant's life. For sample plant 14, Figs. 15 and 16 show the empirical cumulative distributions for the leak and DEGB probabilities, respectively, per plant year. The 10th-, 50th-, and 90th-percentiles for both empirical cumulative distributions are presented in Table 10.

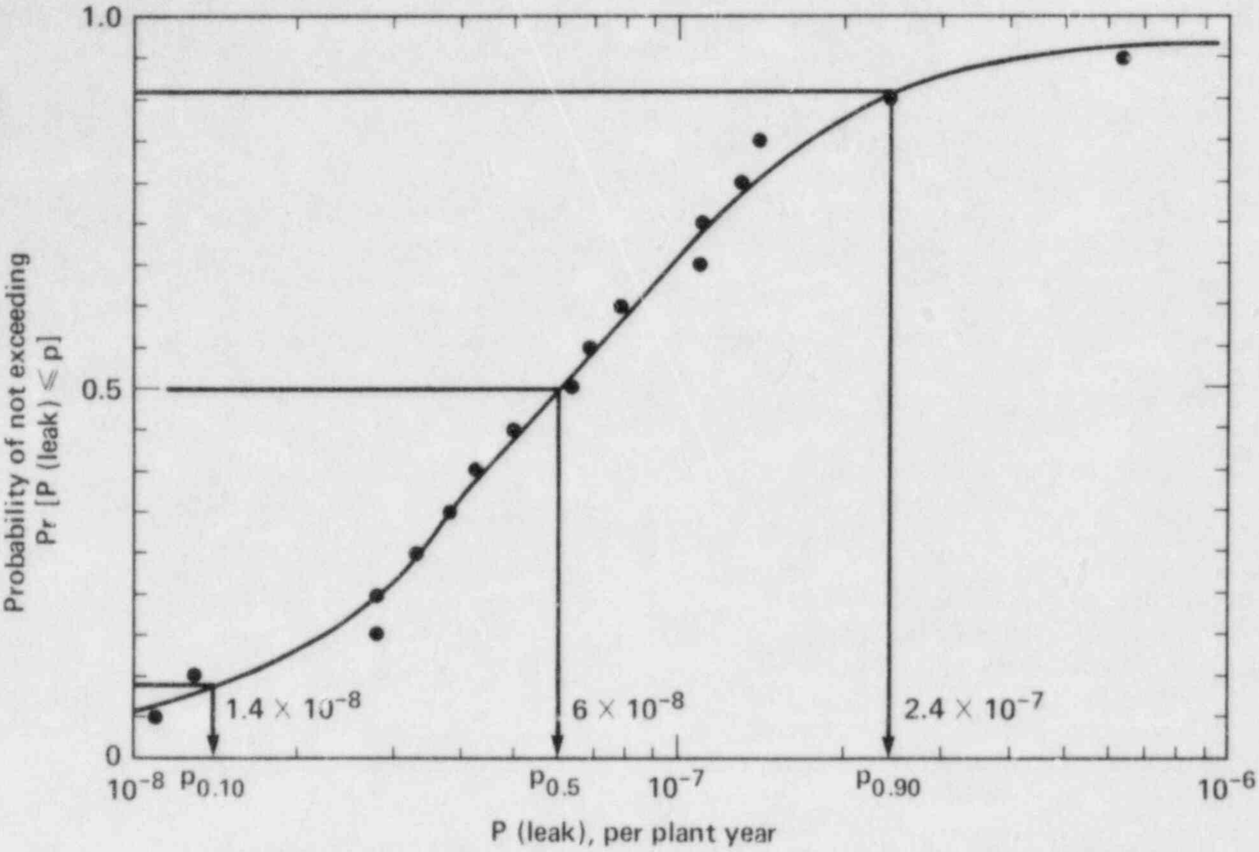

Figure 15. Empirical probability distribution for a cumulative leak in the sample plant having the highest probability for a DEGB.

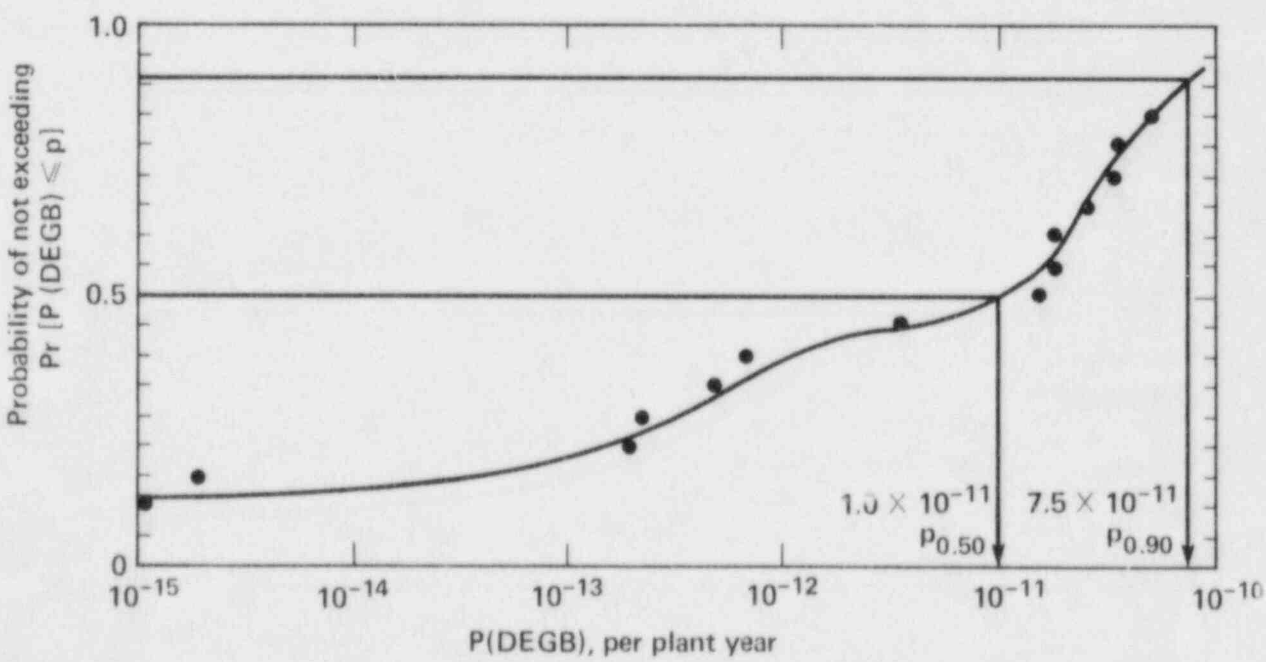

Figure 16. Empirical probability distribution for a cumulative DEGB in the sample plant having the highest probability for a DEGB.

Since sample plant 14 represents the plant with the highest probability for the occurrence of a DEGB, it is reasonable to assume that the 90th-percentiles of its failure probabilities are the greatest for all the plants. The 90th-percentile failure probability for plant 14 can therefore be considered as the upper bound for all the sample plants.

Considering the upper bounds for failure probabilities in the uncertainty analysis, and treating the 17 sample plants as being representative of all of the Westinghouse plants east of the Rocky Mountains, we conclude the following:

(1) We are 90% confident that each Westinghouse plant east of the Rocky Mountains has a probability of a leak in the RCL piping of less than 2.4×10^{-7} per plant year.

(2) We are 90% confident that each Westinghouse plant east of the Rocky Mountains has a probability that a DEGB will occur in the RCL piping of less than 7.5×10^{-11} per plant year.

(3) Differences of at least three orders of magnitude between the leak and DEGB probabilities support the "leak before break" hypothesis for the RCL piping in the Westinghouse plants east of the Rocky Mountains.

Table 10. The 10th-, 50th-, and 90th-percentiles of the empirical failure probabilities for the sample plant with the highest probability for a DEGB.

	Percentile		
	10th	50th	90th
P(leak)	1.4×10^{-8}	6.0×10^{-8}	2.4×10^{-7}
P(DEGB)	$<1.0 \times 10^{-12}$	1.0×10^{-11}	7.5×10^{-11}

6. CONCLUSIONS AND RECOMMENDATIONS

Failure probabilities, estimated by using best-estimate and uncertainty analyses, have been presented for the RCL piping of Westinghouse PWR plants east of the Rocky Mountains. In the best-estimate analysis, point estimates of the probabilities for an RCL piping failure in each of 17 sample plants (representing 33 reactor units at 19 plant sites) were obtained. For those plants, the estimated probabilities for an RCL piping leak ranged from 10^{-8} to 10^{-9} per plant year. The estimated probabilities for a direct DEGB in the RCL piping were estimated as being about 10^{-12} per plant year. In the uncertainty analysis, the uncertainty bounds for the 90th-percentiles of the probabilities for a leak and a direct DEGB were established as being 2.4×10^{-7} and 7.5×10^{-11} respectively, per plant year. Based on the results of both analyses, we conclude:

(1) A direct DEGB is a very unlikely event for the RCL piping of the Westinghouse PWR plants east of the Rocky Mountains.

(2) Earthquakes contribute very little (at most about 1%) to the probability for a direct DEGB in the RCL piping of the Westinghouse PWR plants east of the Rocky Mountains.

(3) The difference of at least three orders of magnitude between the probabilities for a leak or a DEGB suggests that a leak failure is more likely than a direct DEGB failure in the RCL piping of the Westinghouse PWR plants east of the Rocky Mountains.

These conclusions lead us to the following considerations about the design criteria for RCL piping in the Westinghouse PWR plants east of the Rocky Mountains:

(1) The design requirements for simultaneous DEGB and SSE loads (as related to the crack growth mechanism in the RCL piping) should be reconsidered, since the probabilities for the occurrence of these events are extremely low.

(2) Design requirements for postulating failure modes related to the crack growth mechanism in the RCL piping should be focused on the "leak" mode rather than the "DEGB" mode.

REFERENCES

1. "Design Bases for Protection Against Natural Phenomena," Code of Federal Regulations (10 CFR 50, Appendix A) Criterion 2, Office of the Federal Registrar, Washington, D.C. (1983).

2. S. C. Lu, R. D. Steit, and C. K. Chou, "Probability of Pipe Fracture in the Primary Coolant Loop of a PWR Plant," Lawrence Livermore National Laboratory, Livermore, Calif., UCID-18967, Vol. 1, USNRC Report NUREG/CR-2189, Vol. 1, Aug. 1981.[a]

3. "World List of Nuclear Power Plants," Nuclear News, American Nuclear Society, La Grange Park, Ill., Aug. 1983.

4. Letter from R. A. Holmes and E. R. Johnson, Westinghouse Electric Corporation, to C. K. Chou, Lawrence Livermore National Laboratory, "Transmittal of Revised Probabilistic Fracture Mechanics Data Package," Letter PT-SSD-538, Nov. 16, 1982.

5. R. A. Holmes and E. R. Johnson, "Transmittal of Revised Probabilistic Fracture Mechanics Data Package," Water Reactor Division, Westinghouse Electric Corporation, Pittsburgh, Pa., Letter PT-SSD-464 to C. K. Chou, Sept. 1982.

6. D. O. Harris, E. Y. Lim, and D. D. Dedhia, "Probability of Pipe Fracture in the Primary Coolant Loop of a PWR Plant," Lawrence Livermore National Laboratory, Livermore, Calif., UCID-18967, Vol. 5, USNRC Report NUREG/CR-2189, Vol. 5, Aug. 1981.[a]

7. E. Y. Lim, "Probability of Pipe Fracture in the Primary Coolant Loop of a PWR Plant," Lawrence Livermore National Laboratory, Livermore, Calif., UCID-18967, Vol. 9, USNRC Report NUREG/CR-2189, Vol. 9, Aug. 1981.[a]

8. L. L. George and R. W. Mensing, "Probability of Pipe Fracture in the Primary Coolant Loop of a PWR Plant, Vol. 7," Lawrence Livermore National Laboratory, Livermore, Calif., USNRC Report NUREG/CR-2189, Vol. 7, Aug. 1981.[a]

9. L. L. George and R. W. Mensing, Lawrence Livermore National Laboratory, Livermore, Calif. Addendum to Reference 8, (in process).

10. W. Marshall, "An Assessment of the Integrity of PWR Pressure Vessels," Report by a study group under the Chairmanship of W. Marshall, United Kingdom Atomic Energy Authority, H. M. Stationers Office, London, Oct. 1976.

---

[a] Available for purchase from the National Technical Information Service, Springfield, Va. 22161.

11. M. K. Ravindra, R.D. Campbell, R. P. Kennedy, and H. Banon, "Probability of Pipe Failure in the Reactor Coolant Loop of Westinghouse PWR Plants, Vol. 3: Guillotine Break Indirectly Induced by Earthquake," Lawrence Livermore National Laboratory, Livermore, Calif., UCID-19988, USNRC Report, NUREG/CR-3660, Vol. 3, Washington, D.C., Feb. 1984.[a]

12. H. Tada, P. Paris, and R. Gamble, "Stability Analysis of Circumferential Cracks in Reactor Piping Systems," USNRC Report NUREG/CR-0838, Washington, D.C., June 1979.[a]

13. M. F. Kanninen, D. Brock, C. W. Marschall, E. F. Rybicki, S. G. Sampath, F. A. Simonen, and G. M. Wilkowski, "Mechanical Fracture Prediction for Sensitized Stainless Steel Piping with Circumferential Cracks," Battelle report to EPRI, NP-192, Project 585-1, Final Report, Sept. 1976.

14. D. O. Harris, E. Y. Lim, D. D. Dedhia, H. H. Woo, and C. K. Chou, "Fracture Mechanics Models Developed for Piping Reliability Assessment in Light Water Reactors," Lawrence Livermore National Laboratory, Livermore, Calif., UCRL-15490, USNRC Report NUREG/CR-2301, Washington, D.C., April 1982.[a]

15. E. K. Lynn, "The OCTAVIA Code for Predicting Vessel Performance and Failure Probabilities," presented at the Fifth Water Reactor Safety Meeting, Gaithersburg, Md. (1977).

16. P. E. Becher and B. Hansen, "Statistical Evaluation of Defects in Welds and Design Implications," Danish Welding Institute, Danish Atomic Energy Commission Research Establishment, RISO.

17. S. A. Wilson, "Estimating the Relative Probability of Pipe Severance by Fault Cause," General Electric Company, San Jose, Calif., Report GEAP-20615, Sept. 1974.

18. J. J. Johnson, G. L. Goudreau, S. E. Bumpus, and O. R. Moslenikov, "SMACS--Seismic Methodology Analysis Chain with Statistics (Project VIII)", Lawrence Livermore National Laboratory, Livermore, Calif., UCRL-53021, USNRC Report NUREG/CR-2015, Vol. 9, Sept. 1981.[a]

19. Regulatory Guide 1.60, "Design Response Spectra for Seismic Design of Nuclear Power Plants," U. S. Nuclear Regulatory Commission, Washington, D.C., Dec. 1973.

20. Standard Review Plan 3.7.1, "Seismic Design Parameters," USNRC Report NUREG 0800, Washington, D.C., July 1981.[a]

21. Standard Review Plan 3.7.2, "Seismic Systems Analysis," USNRC Report NUREG 0800, Washington, D.C., July, 1981.[a]

---

[a] Available for purchase from the National Technical Information Service, Springfield, Va. 22161.

22. Regulatory Guide 1.122, "Development of Floor Design Response Spectra for Seismic Design of Floor Supported Equipment or Components," U.S. Nuclear Regulatory Commission, Washington, D.C., Feb. 1978.

23. W. J. O'Connell, T. Y. Chuang, R. W. Mensing, P. D. Smith, and J. J. Johnson, "Ranking of Sources of Uncertainty in the SSMRP Seismic Methodology Chain," Lawrence Livermore National Laboratory, Livermore, Calif., UCRL-53027, USNRC Report NUREG/CR-2092, Washington, D.C., June 1981. Available for purchase from the National Technical Information Service, Springfield, Va. 22161.

APPENDIX A. GEOMETRIC AND LOADING INFORMATION FOR THE CIRCUMFERENTIAL WELD JOINTS IN THE RCL PIPING OF 17 SAMPLE PLANTS

Information about the geometries and loadings of the circumferential weld joints of the RCL piping in each of the 17 sample plants of this study is tabulated in this Appendix (Tables A-1 through A-17). The geometric information includes the pipe's inner radius and thickness, its cross-sectional area, and its sectional modulus. Loading information includes the loads from dead weight, the thermal expansion and pipe internal pressure loads, and the seismic loads. The abbreviations used in the tables are defined as follows:

AF	Axial force in thousand pounds (kip).
BM	Bending moment (in.-kip) acting on the plane perpendicular to the pipe axial axis.
KIP	Thousand pounds of load.
KSI	Kips per square inch.
OBE	Operating basis earthquake.
OP	Operating
PEAK G	Acceleration (in g, where g = 386.4 in./s^2) in the horizontal plane.
SIG	Axial stress (σ, in ksi) calculated from the axial force and bending moment.
SSE	Safe shutdown earthquake.

Table A-1. Geometry and loadings for sample plant 1.

PLANT 1 GEOMETRY

WELD	INNER RADIUS (INCHES)	THICKNESS (INCHES)	AREA (IN**2)	SECTION MOD (IN**3)
1	14.50	2.80	279.73	2457.46
2	14.50	2.80	279.73	2457.46
3	14.50	2.80	279.73	2457.46
4	14.50	2.80	279.73	2457.46
5	15.50	3.38	364.47	3506.69
6	15.50	3.31	357.07	3421.92
7	15.50	3.00	320.44	3010.61
8	15.50	3.00	320.44	3010.61
9	15.50	3.00	320.44	3010.61
10	15.50	3.00	320.44	3010.61
11	15.50	3.31	357.07	3421.92
12	13.75	2.70	256.17	2140.92
13	13.75	2.70	256.17	2140.92
14	13.75	2.70	256.17	2140.92
15	13.75	2.70	256.17	2140.92
16	13.75	3.03	290.62	2486.78

PLANT 1 LOADINGS

WELD	**** DEADWEIGHT LOAD *****			****** THERMAL LOAD ******			OP PRESSURE
	AF(KIPS)	BM(IN-K)	SIG(KSI)	AF(KIPS)	BM(IN-K)	SIG(KSI)	(KSI)
1	12.	534.	.26	-6.	24087.	9.78	2.24
2	0.	0.	0.00	0.	0.	0.00	2.24
3	0.	0.	0.00	0.	0.	0.00	2.24
4	4.	184.	.09	-6.	6272.	2.53	2.24
5	10.	144.	.07	-150.	14056.	3.60	2.24
6	26.	213.	.14	-38.	2931.	.75	2.18
7	22.	119.	.11	-42.	2772.	.79	2.18
8	15.	101.	.08	-42.	2905.	.83	2.18
9	4.	370.	.14	-2	1320.	.43	2.18
10	7.	224.	.10	-2.	3191.	1.05	2.18
11	19.	366.	.16	41.	5446.	1.71	2.18
12	7.	23.	.04	9.	4779.	2.27	2.28
13	0.	0.	0.00	0.	0.	0.00	2.28
14	0.	0.	0.00	0.	0.	0.00	2.28
15	6.	81.	.06	9.	3629.	1.73	2.28
16	9.	23.	.04	8.	5114.	2.08	2.28

WELD	*********** OBE LOAD ***********				*********** SSE LOAD ***********			
	PEAK G	AF(KIPS)	BM(IN-K)	SIG(KSI)	PEAK G	AF(KIPS)	BM(IN-K)	SIG(KSI)
1	.06	30.	334.	.24	.12	60.	668.	.49
2	.06	0.	0.	0.00	.12	0.	0.	0.00
3	.06	0.	0.	0.00	.12	0.	0.	0.00
4	.06	30.	158.	.17	.12	60.	316.	.34
5	.06	29.	389.	.19	.12	58.	778.	.38
6	.06	5.	491.	.16	.12	10.	982.	.31
7	.06	6.	331.	.13	.12	12.	662.	.26
8	.06	9.	174.	.09	.12	18.	348.	.17
9	.06	7.	203.	.09	.12	14.	406.	.18
10	.06	5.	178.	.07	.12	10.	356.	.15
11	.06	6.	520.	.17	.12	12.	1040.	.34
12	.06	15.	686.	.38	.12	30.	1372.	.76
13	.06	0.	0.	0.00	.12	0.	0.	0.00
14	.06	0.	0.	0.00	.12	0.	0.	0.00
15	.06	16.	204.	.16	.12	32.	408.	.32
16	.06	15.	469.	.24	.12	30.	938.	.48

Table A-2. Geometry and loadings for sample plant 2.

PLANT 2 GEOMETRY

WELD	INNER RADIUS (INCHES)	THICKNESS (INCHES)	AREA (IN**2)	SECTION MOD (IN**3)
1	14.50	2.45	242.07	2076.58
2	14.50	2.45	242.07	2076.58
3	14.50	2.45	242.07	2076.58
4	14.50	2.45	242.07	2076.58
5	15.50	3.38	364.47	3506.69
6	15.50	3.31	357.07	3421.92
7	15.50	2.60	274.45	2513.69
8	15.50	2.60	274.45	2513.69
9	15.50	2.60	274.45	2513.69
10	15.50	2.60	274.45	2513.69
11	15.50	3.19	342.64	3258.22
12	13.75	2.32	217.34	1767.62
13	13.75	2.32	217.34	1767.62
14	13.75	2.32	217.34	1767.62
15	13.75	2.32	217.34	1767.62
16	13.75	3.03	290.62	2486.78

PLANT 2 LOADINGS

WELD	**** DEADWEIGHT LOAD *****			****** THERMAL LOAD ******			OP PRESSURE
	AF(KIPS)	BM(IN-K)	SIG(KSI)	AF(KIPS)	BM(IN-K)	SIG(KSI)	(KSI)
1	0.	0.	0.00	-15.	21455.	10.27	2.24
2	0.	0.	0.00	0.	0.	0.00	2.24
3	0.	0.	0.00	0.	0.	0.00	2.24
4	0.	0.	0.00	-15.	9518.	4.52	2.24
5	0.	0.	0.00	-200.	17855.	4.54	2.24
6	0.	0.	0.00	-40.	1950.	.46	2.18
7	0.	0.	0.00	-50.	1755.	.52	2.18
8	0.	0.	0.00	-50.	2090.	.65	2.18
9	0.	0.	0.00	-5.	1422.	.55	2.18
10	0.	0.	0.00	-5.	1832.	.71	2.18
11	0.	0.	0.00	38.	4468.	1.48	2.18
12	0.	0.	0.00	15.	11024.	6.31	2.28
13	0.	0.	0.00	0.	0.	0.00	2.28
14	0.	0.	0.00	0.	0.	0.00	2.28
15	0.	0.	0.00	[illegible]	9579.	5.49	2.28
16	0.	0.	0.00	10.	11430	4.63	2.28

WELD	*********** OBE LOAD ***********				*********** [illegible]E LOAD ***********			
	PEAK G	AF(KIPS)	BM(IN-K)	SIG(KSI)	PEAK G	[illegible]	BM(IN-K)	SIG(KSI)
1	.09	259.	5687.	3.81	.18	390.	6659.	[illegible]
2	.09	0.	0.	0.00	.18	0.	0.	[illegible]
3	.09	0.	0.	0.00	.18	0.	[illegible]	0.00
4	.09	254.	7153.	4.49	.18	384.	8343.	5.60
5	.09	250.	10914.	3.80	.18	360.	13168.	4.74
6	.09	88.	5676.	1.91	.18	125.	9508.	3.13
7	.09	88.	4739.	2.21	.18	126.	7619.	3.49
8	.09	87.	3905.	1.87	.18	125.	5302.	2.56
9	.09	107.	3958.	1.96	.18	202.	6413.	3.29
10	.09	105.	6367.	2.92	.18	200.	8053.	3.93
11	.09	122.	11805.	3.98	.18	191.	12017.	[illegible]
12	.09	527.	12634.	9.57	.18	474.	12666.	9.35
13	.09	0.	0.	0.00	.18	0.	0.	0.00
14	.09	0.	0.	0.00	.18	0.	0.	0.00
15	.09	549.	6850.	6.40	.18	484.	6657.	5.99
16	.09	549.	8366.	5.25	.18	485.	8342.	5.02

Table A-3. Geometry and loadings for sample plant 3.

PLANT 3 GEOMETRY

WELD	INNER RADIUS (INCHES)	THICKNESS (INCHES)	AREA (IN**2)	SECTION MOD (IN**3)
1	14.50	2.80	279.73	2457.46
2	14.50	2.80	279.73	2457.46
3	14.50	2.80	279.73	2457.46
4	14.50	2.80	279.73	2457.46
5	15.50	3.38	364.47	3506.69
6	15.50	3.31	357.07	3421.92
7	15.50	3.00	320.44	3010.61
8	15.50	3.00	320.44	3010.61
9	15.50	3.00	320.44	3010.61
10	15.50	3.00	320.44	3010.61
11	15.50	3.31	357.07	3421.92
12	13.75	2.70	256.17	2140.92
13	13.75	2.70	256.17	2140.92
14	13.75	2.70	256.17	2140.92
15	13.75	2.70	256.17	2140.92
16	13.75	3.03	290.62	2486.78

PLANT 3 LOADINGS

WELD	**** DEADWEIGHT LOAD *****			****** THERMAL LOAD ******			OP PRESSURE
	AF(KIPS)	BM(IN-K)	SIG(KSI)	AF(KIPS)	BM(IN-K)	SIG(KSI)	(KSI)
1	11.	475.	.23	-20.	26717.	10.80	2.24
2	0.	0.	0.00	0.	0.	0.00	2.24
3	0.	0.	0.00	0.	0.	0.00	2.24
4	4.	156	.08	-20.	7923.	3.15	2.24
5	9.	215.	.05	-180.	16643.	4.25	2.24
6	26.	164.	.12	-00.	5382.	1.35	2.18
7	21.	117.	.10	-88.	4881.	1.35	2.18
8	15.	84.	.07	-88.	5585.	1.58	2.18
9	4.	224.	.09	-18.	1972.	.60	2.18
10	1.	287.	.10	-18.	2603.	.81	2.18
11	12.	273.	.11	80.	7814.	2.51	2.18
12	8.	53.	.06	8.	4052.	1.92	2.28
13	0.	0.	0.00	0.	0.	0.00	2.28
14	0.	0.	0.00	0.	0.	0.00	2.28
15	11.	717.	.38	8	3651.	1.74	2.28
16	13.	549.	.27	8.	4109.	1.68	2.28

WELD	*********** OBE LOAD ***********				*********** SSE LOAD ***********			
	PEAK G	AF(KIPS)	BM(IN-K)	SIG(KSI)	PEAK G	AF(KIPS)	BM(IN-K)	SIG(KSI)
1	.09	288.	13409.	6.49	.18	115.	7898.	3.63
2	.09	0.	0.	0.00	.18	0.	0.	0.00
3	.09	0.	0.	0.00	.18	0.	0.	0.00
4	.09	286.	13436.	6.49	.18	114.	5907.	2.81
5	.09	285.	16147.	5.39	.18	113.	9390.	2.99
6	.09	128.	13870.	4.41	.18	122.	11764.	3.78
7	.09	130.	10233.	3.80	.18	123.	8055.	3.06
8	.09	129.	6778.	2.65	.18	122.	4254.	1.79
9	.09	124.	9067.	3.40	.18	116.	8609.	3.22
10	.09	121.	11047.	4.05	.18	114.	11061.	4.03
11	.09	117.	10583.	3.42	.18	111.	10546.	3.39
12	.09	340.	17641.	9.57	.18	135.	12732.	6.47
13	.09	0.	0.	0.00	.18	0.	0.	0.00
14	.09	0.	0.	0.00	.18	0.	0.	0.00
15	.09	349.	10732.	6.38	.18	242.	10077.	5.65
16	.09	349.	12753.	6.33	.18	242.	11585.	5.49

Table A-4. Geometry and loadings for sample plant 4.

PLANT 4 GEOMETRY

WELD	INNER RADIUS (INCHES)	THICKNESS (INCHES)	AREA (IN**2)	SECTION MOD (IN**3)
1	14.50	2.45	242.07	2076.58
2	14.50	2.45	242.07	2076.58
3	14.50	2.45	242.07	2076.58
4	14.50	2.45	242.07	2076.58
5	15.50	3.38	364.47	3506.69
6	15.50	3.31	357.07	3421.92
7	15.50	2.60	274.45	2513.69
8	15.50	2.60	274.45	2513.69
9	15.50	2.60	274.45	2513.69
10	15.50	2.60	274.45	2513.69
11	15.50	3.19	342.64	3258.22
12	13.75	2.32	217.34	1767.62
13	13.75	2.32	217.34	1767.62
14	13.75	2.32	217.34	1767.62
15	13.75	2.32	217.34	1767.62
16	13.75	3.03	290.62	2486.78

PLANT 4 LOADINGS

WELD	**** DEADWEIGHT LOAD *****			****** THERMAL LOAD ******			OP PRESSURE
	AF(KIPS)	BM(IN-K)	SIG(KSI)	AF(KIPS)	BM(IN-K)	SIG(KSI)	(KSI)
1	43.	1123.	.72	-1.	11909.	5.73	2.24
2	0.	0.	0.00	0.	0.	0.00	2.24
3	0.	0.	0.00	0.	0.	0.00	2.24
4	43.	168.	.26	-1.	6500.	3.13	2.24
5	255.	992.	.98	-73.	10618.	2.83	2.24
6	18.	1659.	.54	-36.	2394.	.60	2.18
7	18.	1792.	.78	-43.	2214.	.72	2.18
8	18.	2150.	.92	-43.	2777.	.95	2.18
9	6.	3047.	1.23	-9.	1400.	.52	2.18
10	6.	4360.	1.76	-9.	592.	.20	2.18
11	24.	4989.	1.60	43.	4056.	1.37	2.18
12	62.	835.	.76	3.	4234.	2.41	2.28
13	0.	0.	0.00	0.	0.	0.00	2.28
14	0.	0.	0.00	0.	0.	0.00	2.28
15	62.	848.	.77	3.	4067.	2.31	2.28
16	59.	943.	.58	1.	4768.	1.92	2.28

WELD	*********** OBE LOAD ***********				*********** SSE LOAD ***********			
	PEAK G	AF(KIPS)	BM(IN-K)	SIG(KSI)	PEAK G	AF(KIPS)	BM(IN-K)	SIG(KSI)
1	.06	319	3348.	2.93	.10	563.	8134.	6.24
2	.06	0.	0.	0.00	.10	0.	0.	0.00
3	.06	0.	0.	0.00	.10	0.	0.	0.00
4	.06	317.	2682.	2.60	.10	555.	6732.	5.53
5	.06	194.	7946.	2.80	.10	342.	14118.	4.96
6	.06	58.	8819.	2.74	.10	115.	16336.	5.10
7	.06	64.	5923.	2.59	.10	120.	11029.	4.82
8	.06	64.	1858.	.97	.10	119.	4676.	2.29
9	.06	84.	2886.	1.45	.10	157.	5291.	2.68
10	.06	83.	4771.	2.20	.10	154.	9113.	4.19
11	.06	108.	7359.	2.57	.10	318.	23101.	8.02
12	.06	253.	6902.	5.07	.10	532.	19346.	13.39
13	.06	0.	0.	0.00	.10	0.	0.	0.00
14	.06	0.	0.	0.00	.10	0.	0.	0.00
15	.06	253.	2328.	2.48	.10	528.	6595.	6.16
16	.06	243.	3200.	2.12	.10	508.	8914.	5.33

Table A-5. Geometry and loadings for sample plant 5.

PLANT 5 GEOMETRY

WELD	INNER RADIUS (INCHES)	THICKNESS (INCHES)	AREA (IN**2)	SECTION MOD (IN**3)
1	14.50	2.45	242.07	2076.58
2	14.50	2.45	242.07	2076.58
3	14.50	2.45	242.07	2076.58
4	14.50	2.45	242.07	2076.58
5	15.50	3.38	364.47	3506.69
6	15.50	3.31	357.07	3421.92
7	15.50	2.60	274.45	2513.69
8	15.50	2.60	274.45	2513.69
9	15.50	2.60	274.45	2513.69
10	15.50	2.60	274.45	2513.69
11	15.50	3.19	342.64	3258.22
12	13.75	2.32	217.34	1767.62
13	13.75	2.32	217.34	1767.62
14	13.75	2.32	217.34	1767.62
15	13.75	2.32	217.34	1767.62
16	13.75	3.03	290.62	2486.78

PLANT 5 LOADINGS

WELD	**** DEADWEIGHT LOAD *****			****** THERMAL LOAD ******			OP PRESSURE
	AF(KIPS)	BM(IN-K)	SIG(KSI)	AF(KIPS)	BM(IN-K)	SIG(KSI)	(KSI)
1	9.	300.	.18	-35.	30686.	14.63	2.24
2	0.	0.	0.00	0.	0.	0.00	2.24
3	0.	0.	0.00	0.	0.	0.00	2.24
4	4.	110.	.07	-35.	13685.	6.45	2.24
5	11.	225.	.09	-200.	25344.	6.68	2.24
6	11.	270.	.11	-80.	5898.	1.50	2.18
7	18.	59.	.09	-90.	5014.	1.67	2.18
8	13.	50.	.07	-90.	5000.	1.66	2.18
9	1.	261.	.11	-15.	1802.	66	2.18
10	3.	213.	.10	-15.	3893.	1.49	2.18
11	20.	261.	.14	80.	8354.	2.80	2.18
12	10.	306.	.22	15.	10344.	5.92	2.28
13	0.	0.	0.00	0.	0.	0.00	2.28
14	0.	0.	0.00	0.	0.	0.00	2.28
15	-1.	150.	.08	15.	9012.	5.17	2.28
16	-1.	326.	.13	15.	10733.	4.37	2.28

WELD	*********** OBE LOAD ***********				*********** SSE LOAD ***********			
	PEAK G	AF(KIPS)	BM(IN-K)	SIG(KSI)	PEAK G	AF(KIPS)	BM(IN-K)	SIG(KSI)
1	.06	581.	10315.	7.37	.12	574.	13604.	8.92
2	.06	0.	0.	0.00	.12	0.	0.	0.00
3	.06	0.	0.	0.00	.12	0.	0.	0.00
4	.06	576.	4974.	4.77	.12	568.	6667.	5.56
5	.06	372.	11762.	4.37	.12	369.	13240.	4.79
6	.06	149.	21702.	6.76	.12	207.	28174.	8.81
7	.06	42.	13678.	5.59	.12	77.	17794.	7.36
8	.06	42.	5754.	2.44	.12	77.	7496.	3.26
9	.06	218.	11466.	5.36	.12	277.	14231.	6.67
10	.06	214.	11551.	5.37	.12	70.	14103.	5.87
11	.06	42.	8515.	2.74	.12	79.	11225.	3.68
12	.06	232.	12746.	8.28	.12	329.	15188.	10.11
13	.06	0.	0.	0.00	.12	0.	0.	0.00
14	.06	0.	0.	0.00	.12	0.	0.	0.00
15	.06	238.	9780.	6.63	.12	338.	13010.	8.92
16	.06	213.	11425.	5.33	.12	304.	15238.	7.17

Table A-6. Geometry and loadings for sample plant 6.

PLANT 6 GEOMETRY

WELD	INNER RADIUS (INCHES)	THICKNESS (INCHES)	AREA (IN**2)	SECTION MOD (IN**3)
1	14.50	2.45	242.07	2076.58
2	14.50	2.45	242.07	2076.58
3	14.50	2.45	242.07	2076.58
4	14.50	2.45	242.07	2076.58
5	15.50	3.38	364.47	3506.69
6	15.50	3.31	357.07	3421.92
7	15.50	2.60	274.45	2513.69
8	15.50	2.60	274.45	2513.69
9	15.50	2.60	274.45	2513.69
10	15.50	2.60	274.45	2513.69
11	15.50	3.19	342.64	3258.22
12	13.75	2.32	217.34	1767.62
13	13.75	2.32	217.34	1767.62
14	13.75	2.32	217.34	1767.62
15	13.75	2.32	217.34	1767.62
16	13.75	3.03	290.62	2486.78

PLANT 6 LOADINGS

WELD	**** DEADWEIGHT LOAD *****			****** THERMAL LOAD ******			OP PRESSURE
	AF(KIPS)	BM(IN-K)	SIG(KSI)	AF(KIPS)	BM(IN-K)	SIG(KSI)	(KSI)
1	1.	723.	.35	-22.	25464.	12.17	2.24
2	0.	0.	0.00	0.	0.	0.00	2.24
3	0.	0.	0.00	0.	0.	0.00	2.24
4	1.	284.	.14	-22.	10841.	5.13	2.24
5	6.	135.	.05	-193	20536.	5.33	2.24
6	16.	45.	.06	-78.	6180.	1.59	2.18
7	15.	186.	.13	-92	5275.	1.76	2.18
8	10.	168.	.10	-92.	5380.	1.81	2.18
9	1.	281.	.12	-2.	1670.	.66	2.18
10	1.	126.	.05	-2.	3996.	1.58	2.18
11	23.	484.	.22	92.	8922.	3.01	2.18
12	-1.	201.	.11	18.	6506.	3.76	2.28
13	0.	0.	0.00	0.	0.	0.00	2.28
14	0.	0.	0.00	0.	0.	0.00	2.28
15	-1.	257.	.14	18.	5889.	3.41	2.28
16	-1.	429.	.17	16.	6957.	2.85	2.28

WELD	************ OBE LOAD ************				************ SSE LOAD ************			
	PEAK G	AF(KIPS)	BM(IN-K)	SIG(KSI)	PEAK G	AF(KIPS)	BM(IN-K)	SIG(KSI)
1	.12	247.	7078.	4.43	.20	383.	9607.	6.21
2	.12	0.	0.	0.00	.20	0.	0.	0.00
3	.12	0.	0.	0.00	.20	0.	0.	0.00
4	.12	238.	9193.	5.41	.20	370.	10934.	6.79
5	.12	167.	104.	.49	.20	259.	13073.	4.44
6	.12	113.	12596.	4.00	.20	159.	17643.	5.60
7	.12	114.	8130.	3.65	.20	168.	11841.	5.32
8	.12	114.	3138.	1.66	.20	168.	4419.	2.37
9	.12	226.	7473.	3.80	.20	296.	9762.	4.96
10	.12	227.	11254.	5.30	.20	296.	14498.	6.85
11	.12	99.	5272.	1.91	.20	127.	7309.	2.61
12	.12	307.	9976.	7.06	.20	426.	13753.	9.74
13	.12	0.	0.	0.00	.20	0.	0.	0.00
14	.12	0.	0.	0.00	.20	0.	0.	0.00
15	.12	315.	6569.	5.17	.20	439.	8714.	6.95
16	.12	289.	7941.	4.19	.20	402.	10579.	5.64

Table A-7. Geometry and loadings for sample plant 7.

PLANT 7 GEOMETRY

WELD	INNER RADIUS (INCHES)	THICKNESS (INCHES)	AREA (IN**2)	SECTION MOD (IN**3)
1	14.50	2.45	242.07	2076.58
2	14.50	2.45	242.07	2076.58
3	14.50	2.45	242.07	2076.58
4	14.50	2.45	242.07	2076.58
5	15.50	3.38	364.47	3506.69
6	15.50	3.31	357.07	3421.92
7	15.50	2.60	274.45	2513.69
8	15.50	2.60	274.45	2513.69
9	15.50	2.60	274.45	2513.69
10	15.50	2.60	274.45	2513.69
11	15.50	3.19	342.64	3258.22
12	13.75	2.32	217.34	1767.62
13	13.75	2.32	217.34	1767.62
14	13.75	2.32	217.34	1767.62
15	13.75	2.32	217.34	1767.62
16	13.75	3.03	290.62	2486.78

PLANT 7 LOADINGS

WELD	**** DEADWEIGHT LOAD *****			****** THERMAL LOAD ******			OP PRESSURE
	AF(KIPS)	BM(IN-K)	SIG(KSI)	AF(KIPS)	BM(IN-K)	SIG(KSI)	(KSI)
1	12.	566.	.32	-38.	28193.	13.42	2.24
2	0.	0.	0.00	0.	0.	0.00	2.24
3	0.	0.	0.00	0.	0.	0.00	2.24
4	2.	181.	.10	-38.	8080.	3.73	2.24
5	-10.	79.	-.00	-185.	17154.	4.38	2.24
6	20.	73.	.08	-98.	3027.	.61	2.18
7	16.	209.	.14	-91.	3107.	.90	2.18
8	10.	143.	.09	-91.	4724.	1.55	2.18
9	2.	233.	.10	-31.	2448.	.86	2.18
10	5.	105.	.06	-31.	3536.	1.29	2.18
11	17.	344.	.16	91.	9579.	3.21	2.18
12	19.	730.	.50	26.	8919.	5.17	2.28
13	0.	0.	0.00	0.	0.	0.00	2.28
14	0.	0.	0.00	0.	0.	0.00	2.28
15	9.	213.	.16	14.	7684.	4.41	2.28
16	10.	383.	.19	14.	9108.	3.71	2.28

WELD	*********** OBE LOAD ***********				*********** SSE LOAD ***********			
	PEAK G	AF(KIPS)	BM(IN-K)	SIG(KSI)	PEAK G	AF(KIPS)	BM(IN-K)	SIG(KSI)
1	.10	50.	1468.	.91	.20	107.	1758.	1.29
2	.10	0.	0.	0.00	.20	0.	0.	0.00
3	.10	0.	0.	0.00	.20	0.	0.	0.00
4	.10	50.	033.	.51	.20	105.	970.	.90
5	.10	50.	1582.	.59	.20	121.	3055.	1.20
6	.10	8.	770.	.25	.20	13.	1343.	.43
7	.10	11.	674.	.31	.20	16.	915.	42
8	.10	105.	539.	.60	.20	17.	680.	.33
9	.10	14.	450.	.23	.20	20.	765.	.38
10	.10	15.	523.	.26	.20	21.	846.	.41
11	.10	15.	1132.	.39	.20	23.	1361.	.48
12	.10	17.	317.	.26	.20	25.	3913.	2.33
13	.10	0.	0.	0.00	.20	0.	0.	0.00
14	.10	0.	0.	0.00	.20	0.	0.	0.00
15	.10	18.	353.	.28	.20	33.	620.	.50
16	.10	17.	463.	.24	.20	33.	706.	.40

Table A-8. Geometry and loadings for sample plant 8.

PLANT 8 GEOMETRY

WELD	INNER RADIUS (INCHES)	THICKNESS (INCHES)	AREA (IN**2)	SECTION MOD (IN**3)
1	14.50	2.45	242.07	2076.58
2	14.50	2.45	242.07	2076.58
3	14.50	2.45	242.07	2076.58
4	14.50	2.45	242.07	2076.58
5	15.50	3.38	364.47	3506.69
6	15.50	3.31	357.07	3421.92
7	15.50	2.60	274.45	2513.69
8	15.50	2.60	274.45	2513.69
9	15.50	2.60	274.45	2513.69
10	15.50	2.60	274.45	2513.69
11	15.50	3.19	342.64	3258.22
12	13.75	2.32	217.34	1767.62
13	13.75	2.32	217.34	1767.62
14	13.75	2.32	217.34	1767.62
15	13.75	2.32	217.34	1767.62
16	13.75	3.03	290.62	2486.78

PLANT 8 LOADINGS

WELD	**** DEADWEIGHT LOAD *****			****** THERMAL LOAD ******			OP PRESSURE
	AF(KIPS)	BM(IN-K)	SIG(KSI)	AF(KIPS)	BM(IN-K)	SIG(KSI)	(KSI)
1	25.	581.	.38	-23.	16478.	7.84	2.24
2	15.	353.	.23	-23.	1779.	.76	2.24
3	16.	336.	.23	-23.	3588.	1.63	2.24
4	18.	218.	.18	-23.	10087.	4.76	2.24
5	23.	100.	.09	-25.	14296.	4.01	2.24
6	18.	90.	.08	-68.	5210.	1.33	2.18
7	14.	260.	.15	-75.	4300.	1.44	2.18
8	9.	233.	.13	-75.	4118.	1.36	2.18
9	2.	293.	.12	-8.	1563.	.59	2.18
10	6.	159.	.09	-8.	3558.	1.39	2.18
11	19.	272.	.14	68.	6885.	2.31	2.18
12	28.	248.	.27	12.	5977.	3.44	2.28
13	25.	251.	.26	12.	4977.	2.87	2.28
14	3.	754.	.44	12.	2610.	1.53	2.28
15	17.	489.	.35	12.	4064.	2.35	2.28
16	20.	809.	.39	10.	4671.	1.91	2.28

WELD	*********** OBE LOAD ***********				*********** SSE LOAD ***********			
	PEAK G	AF(KIPS)	BM(IN-K)	SIG(KSI)	PEAK G	AF(KIPS)	BM(IN-K)	SIG(KSI)
1	.08	838.	7137.	6.90	.20	1288.	13400.	11.77
2	.08	825.	5391.	6.00	.20	1268.	8457.	9.31
3	.08	797.	9419.	7.83	.20	1224.	14681.	12.13
4	.08	797.	10169.	8.19	.20	1224.	15817.	12.67
5	.08	529.	12063.	4.89	.20	824.	18802.	7.62
6	.08	171.	14916.	4.84	.20	260.	26942.	8.60
7	.08	111.	9848.	4.32	.20	170.	17419.	7.55
8	.08	113.	5039.	2.42	.20	173.	7989.	3.81
9	.08	145.	6209.	3.00	.20	267.	12032.	5.76
10	.08	127.	6094.	2.89	.20	194.	12704.	5.76
11	.08	117.	15589.	5.13	.20	180.	23779.	7.82
12	.08	587.	18191.	12.99	.20	918.	27690.	19.89
13	.08	587.	16213.	11.87	.20	918.	22746.	17.09
14	.08	608.	10957.	9.00	.20	957.	16774.	13.89
15	.08	610.	6175.	6.30	.20	963.	10585.	10.42
16	.08	566.	8289.	5.28	.20	893.	13851.	8.64

Table A-9. Geometry and loadings for sample plant 9.

PLANT 9 GEOMETRY

WELD	INNER RADIUS (INCHES)	THICKNESS (INCHES)	AREA (IN**2)	SECTION MOD (IN**3)
1	14.50	2.45	242.07	2076.58
2	14.50	2.45	242.07	2076.58
3	14.50	2.45	242.07	2076.58
4	14.50	2.45	242.07	2076.58
5	15.50	3.38	364.47	3506.69
6	15.50	3.31	357.07	3421.92
7	15.50	2.60	274.45	2513.69
8	15.50	2.60	274.45	2513.69
9	15.50	2.60	274.45	2513.69
10	15.50	2.60	274.45	2513.69
11	15.50	3.19	342.64	3258.22
12	13.75	2.32	217.34	1767.62
13	13.75	2.32	217.34	1767.62
14	13.75	2.32	217.34	1767.62
15	13.75	2.32	217.34	1767.62
16	13.75	3.03	290.62	2486.78

PLANT 9 LOADINGS

WELD	**** DEADWEIGHT LOAD *****			****** THERMAL LOAD ******			OP PRESSURE
	AF(KIPS)	BM(IN-K)	SIG(KSI)	AF(KIPS)	BM(IN-K)	SIG(KSI)	(KSI)
1	11.	498.	.29	-2.	22531.	10.84	2.24
2	0.	0.	0.00	0.	0.	0.00	2.24
3	0.	0.	0.00	0.	0.	0.00	2.24
4	11.	205.	.14	-2.	6450.	3.10	2.24
5	10.	168.	.08	-182.	13881.	3.46	2.24
6	25.	209.	.13	-41.	2922.	.74	2.18
7	20.	112.	.12	-50.	2762.	.92	2.18
8	14.	95.	.09	-50.	2886.	.97	2.18
9	3.	355.	.15	-9.	1276.	.47	2.18
10	6.	271.	.13	-9.	3156.	1.22	2.18
11	18.	360.	.16	50.	5404.	1.80	2.18
12	6.	98.	.08	10.	4610.	2.65	2.28
13	0.	0.	0.00	0.	0.	0.00	2.28
14	0.	0.	0.00	0.	0.	0.00	2.28
15	5.	75.	.07	10.	3547.	2.05	2.28
16	8.	221.	.12	5.	5004.	2.03	2.28

WELD	*********** OBE LOAD ***********				*********** SSE LOAD ***********			
	PEAK G	AF(KIPS)	BM(IN-K)	SIG(KSI)	PEAK G	AF(KIPS)	BM(IN-K)	SIG(KSI)
1	.06	81.	2237.	1.41	.12	162.	4474.	2.82
2	.06	0.	0.	0.00	.12	0.	0.	0.00
3	.06	0.	0.	0.00	.12	0.	0.	0.00
4	.06	81.	972.	.80	.12	162.	1944.	1.61
5	.06	79.	1818.	.74	.12	158.	3636.	1.47
6	.06	18.	1222.	.41	.12	36.	2444.	.82
7	.06	19.	869.	.41	.12	38.	1738	.83
8	.06	16.	651.	.32	.12	32.	1302.	.63
9	.06	17.	852.	.40	.12	34.	1704.	.80
10	.06	18.	589.	.30	.12	36.	1178.	.60
11	.06	18.	1849.	.62	.12	36.	3698.	1.24
12	.06	45.	2008.	1.34	.12	90.	4016.	2.69
13	.06	0.	0.	0.00	.12	0.	0.	0.00
14	.06	0.	0.	0.00	.12	0.	0.	0.00
15	.06	46.	498.	.49	.12	92.	996.	.39
16	.06	46.	849.	.50	.12	92.	1698.	1.00

Table A-10. Geometry and loadings for sample plant 10.

PLANT 10 GEOMETRY

WELD	INNER RADIUS (INCHES)	THICKNESS (INCHES)	AREA (IN**2)	SECTION MOD (IN**3)
1	14.50	2.80	279.73	2457.46
2	14.50	2.80	279.73	2457.46
3	14.50	2.80	279.73	2457.46
4	14.50	2.80	279.73	2457.46
5	15.50	3.38	364.47	3506.69
6	15.50	3.31	357.07	3421.92
7	15.50	3.00	320.44	3010.61
8	15.50	3.00	320.44	3010.61
9	15.50	3.00	320.44	3010.61
10	15.50	3.00	320.44	3010.61
11	15.50	3.31	357.07	3421.92
12	13.75	2.70	256.17	2140.92
13	13.75	2.70	256.17	2140.92
14	13.75	2.70	256.17	2140.92
15	13.75	2.70	256.17	2140.92
16	13.75	3.03	290.62	2486.78

PLANT 10 LOADINGS

WELD	**** DEADWEIGHT LOAD *****			****** THERMAL LOAD ******			OP PRESSURE
	AF(KIPS)	BM(IN-K)	SIG(KSI)	AF(KIPS)	BM(IN-K)	SIG(KSI)	(KSI)
1	1.	1584.	.65	-248.	11700.	3.87	2.24
2	1.	1368.	.56	-235.	1236.	-.34	2.24
3	1.	1188.	.49	-243.	7516.	2.19	2.24
4	1.	1032.	.42	-243.	6292.	2.51	2.24
5	23.	696.	.26	-231.	8520.	1.80	2.24
6	16.	696.	.25	-88.	7572.	1.97	2.18
7	17.	768.	.31	-103.	5736.	1.58	2.18
8	10.	780.	.29	-103.	5064.	1.36	2.18
9	1.	312.	.11	-11.	840.	.24	2.18
10	1.	216.	.07	-11.	3756.	1.21	2.18
11	28.	1368.	.48	103.	8532.	2.78	2.18
12	1.	1704.	.80	46.	5640.	2.81	2.28
13	1.	288.	.14	46.	4476.	2.27	2.28
14	1.	1272.	.60	47.	2808.	1.50	2.28
15	1.	132.	.07	47.	1394.	.83	2.28
16	1.	468.	.19	31.	1764.	.82	2.28

WELD	*********** OBE LOAD ***********				*********** SSE LOAD ***********			
	PEAK G	AF(KIPS)	BM(IN-K)	SIG(KSI)	PEAK G	AF(KIPS)	BM(IN-K)	SIG(KSI)
1	.06	114.	1140.	.87	.13	159.	1800.	1.30
2	.06	114.	876.	[illegible]	.13	160.	1260.	1.08
3	.06	114.	1594.	1.05	.13	159.	2304.	1.51
4	.06	114.	1668.	1.09	.13	159.	2412.	1.55
5	.06	73.	3306.	1.17	.13	106.	3900.	1.40
6	.06	10.	3636.	1.09	.13	16.	4224.	1.28
7	.06	15.	3024.	1.05	.13	20.	3576.	1.25
8	.06	15.	2052.	.73	.13	20.	1980.	.72
9	.06	22.	648.	.26	.13	27.	876.	.38
10	.06	22.	876.	.36	.13	27.	1068.	.44
11	.06	16.	1164.	.38	.13	22.	1644.	.54
12	.06	18.	636.	.37	.13	31.	1008.	.59
13	.06	18.	504.	.31	.13	31.	792.	.49
14	[illegible]	[illegible]	492.	.30	.13	33.	732.	.47
15	.06	20.	264.	.20	.13	35.	384.	.32
16	.06	17.	288.	.17	.13	29.	432.	.27

Table A-11. Geometry and loadings for sample plant 11.

PLANT 11 GEOMETRY

WELD	INNER RADIUS (INCHES)	THICKNESS (INCHES)	AREA (IN**2)	SECTION MOD (IN**3)
1	14.50	2.45	242.07	2076.58
2	14.50	2.45	242.07	2076.58
3	14.50	2.45	242.07	2076.58
4	14.50	2.45	242.07	2076.58
5	15.50	3.38	364.47	3506.69
6	15.50	3.31	357.07	3421.92
7	15.50	2.60	274.45	2513.69
8	15.50	2.60	274.45	2513.69
9	15.50	2.60	274.45	2513.69
10	15.50	2.60	274.45	2513.69
11	15.50	3.19	342.64	3258.22
12	13.75	2.32	217.34	1767.62
13	13.75	2.32	217.34	1767.62
14	13.75	2.32	217.34	1767.62
15	13.75	2.32	217.34	1767.62
16	13.75	3.03	290.62	2486.78

PLANT 11 LOADINGS

WELD	**** DEADWEIGHT LOAD *****			****** THERMAL LOAD ******			OP PRESSURE
	AF(KIPS)	BM(IN-K)	SIG(KSI)	AF(KIPS)	BM(IN-K)	SIG(KSI)	(KSI)
1	12.	526.	.30	-45	31385.	14.93	2.24
2	0.	0.	0.00	0.	0.	0.00	2.24
3	0.	0.	0.00	0.	0.	0.00	2.24
4	3.	167.	.09	-45.	9305.	4.30	2.24
5	9.	79.	.05	-215.	19742.	5.04	2.24
6	20.	158.	.10	-111.	8769.	2.25	2.18
7	16.	87.	.09	-130.	7513.	2.52	2.18
8	12.	70.	.07	-130.	7900.	2.67	2.18
9	1.	279.	.11	-43.	2223.	.73	2.18
10	3	244.	.11	-43.	5940.	2.21	2.18
11	16.	282.	.13	120.	13438.	4.47	2.18
12	9.	250.	.18	52.	5858.	3.55	2.28
13	0.	0.	0.00	0.	0.	0.00	2.28
14	0.	0.	0.00	0.	0.	0.00	2.28
15	9.	222.	.17	52.	4756.	2.93	2.28
16	11.	443.	.22	30.	7106.	2.96	2.28

WELD	*********** OBE LOAD ***********				*********** SSE LOAD ***********			
	PEAK G	AF(KIPS)	BM(IN-K)	SIG(KSI)	PEAK G	AF(KIPS)	BM(IN-K)	SIG(KSI)
1	.10	206.	6427.	3.95	.15	221.	6918.	4.24
2	.10	0.	0.	0.00	.15	0.	0.	0.00
3	.10	0.	0.	0.00	.15	0.	0.	0.00
4	.10	204.	4304.	2.92	.15	220.	4622.	3.13
5	.10	200.	6818.	2.49	.15	216.	7378.	2.70
6	.10	143.	38307.	11.60	.15	86.	6857.	2.24
7	.10	77.	4430.	2.04	.15	86.	4812.	2.23
8	.10	77.	3270.	1.58	.15	86.	3515.	1.71
9	.10	285.	3247.	2.33	.15	82.	3655.	1.75
10	.10	72.	2500.	1.26	.15	81.	2895.	1.45
11	.10	69.	4353.	1.54	.15	77.	4767.	1.69
12	.10	158.	4196.	3.10	.15	185.	4922.	3.64
13	.10	0.	0.	0.00	.15	0.	0.	0.00
14	.10	0.	0.	0.00	.15	0.	0.	0.00
15	.10	162.	2029.	1.89	.15	189.	2381.	2.22
16	.10	162.	2370.	1.51	.15	189.	2719.	1.74

Table A-12. Geometry and loadings for sample plant 12.

PLANT 12 GEOMETRY

WELD	INNER RADIUS (INCHES)	THICKNESS (INCHES)	AREA (IN**2)	SECTION MOD (IN**3)
1	14.50	2.45	242.07	2076.58
2	14.50	2.45	242.07	2076.58
3	14.50	2.45	242.07	2076.58
4	14.50	2.45	242.07	2076.58
5	15.50	3.38	364.47	3506.69
6	15.50	3.31	357.07	3421.92
7	15.50	2.60	274.45	2513.69
8	15.50	2.60	274.45	2513.69
9	15.50	2.60	274.45	2513.69
10	15.50	2.60	274.45	2513.69
11	15.50	3.19	342.64	3258.22
12	13.75	2.32	217.34	1767.62
13	13.75	2.32	217.34	1767.62
14	13.75	2.32	217.34	1767.62
15	13.75	2.32	217.34	1767.62
16	13.75	3.03	290.62	2486.78

PLANT 12 LOADINGS

WELD	**** DEADWEIGHT LOAD *****			****** THERMAL LOAD ******			OP PRESSURE
	AF(KIPS)	BM(IN-K)	SIG(KSI)	AF(KIPS)	BM(IN-K)	SIG(KSI)	(KSI)
1	9.	280.	.17	-25.	15124.	7.18	2.24
2	0.	0.	0.00	0.	0.	0.00	2.24
3	0.	0.	0.00	0.	0.	0.00	2.24
4	4.	115.	.07	-25.	7009.	3.27	2.24
5	11.	211.	.09	-140.	12989.	3.32	2.24
6	22.	188.	.12	-80.	5478.	1.38	2.18
7	17.	83.	.09	-90.	4680.	1.53	2.18
8	12.	63.	.07	-90.	4916.	1.63	2.18
9	1.	270.	.11	-10.	990.	.36	2.18
10	3.	216.	.10	-10.	3540.	1.37	2.18
11	20.	252.	.14	80.	8449.	2.83	2.18
12	10.	313.	.22	20.	2230.	1.35	2.28
13	0.	0.	0.00	0.	0.	0.00	2.28
14	0.	0.	0.00	0.	0.	0.00	2.28
15	8.	109.	.10	20.	2068.	1.26	2.28
16	10.	273.	.14	20.	2355.	1.02	2.28

WELD	*********** OBE LOAD ***********				*********** SSE LOAD ***********			
	PEAK G	AF(KIPS)	BM(IN-K)	SIG(KSI)	PEAK G	AF(KIPS)	BM(IN-K)	SIG(KSI)
1	.08	239.	6441.	4.09	.15	449.	12077.	7.67
2	.08	0.	0.	0.00	.15	0.	0.	0.00
3	.08	0.	0.	0.00	.15	0.	0.	0.00
4	.08	239.	3249.	2.55	.15	448.	6091.	4.78
5	.08	154.	6823.	2.37	.15	288.	12794.	4.44
6	.08	124.	24729.	7.57	.15	233.	46366.	14.20
7	.08	94.	15514.	6.51	.15	177.	29089.	12.22
8	.08	94.	1428.	.91	.15	177.	2677.	1.71
9	.08	220.	13813.	6.30	.15	412.	25899.	11.80
10	.08	218.	14925.	6.73	.15	408.	27985.	12.62
11	.08	94.	12511.	4.11	.15	176.	23458.	7.71
12	.08	69.	8469.	5.11	.15	130.	15879.	9.58
13	.08	0.	0.	0.00	.15	0.	0.	0.00
14	.08	0.	0.	0.00	.15	0.	0.	0.00
15	.08	70.	10334.	6.17	.15	131.	19376.	11.56
16	.08	53.	11505.	4.81	.15	99.	21572.	9.02

Table A-13. Geometry and loadings for sample plant 13.

PLANT 13 GEOMETRY

WELD	INNER RADIUS (INCHES)	THICKNESS (INCHES)	AREA (IN**2)	SECTION MOD (IN**3)
1	14.50	2.45	242.07	2076.58
2	14.50	2.45	242.07	2076.58
3	14.50	2.45	242.07	2076.58
4	14.50	2.45	242.07	2076.58
5	15.50	3.38	364.47	3506.69
6	15.50	3.31	357.07	3421.92
7	15.50	2.60	274.45	2513.69
8	15.50	2.60	274.45	2513.69
9	15.50	2.60	274.45	2513.69
10	15.50	2.60	274.45	2513.69
11	15.50	3.19	342.64	3258.22
12	13.75	2.32	217.34	1767.62
13	13.75	2.32	217.34	1767.62
14	13.75	2.32	217.34	1767.62
15	13.75	2.32	217.34	1767.62
16	13.75	3.03	290.62	2486.78

PLANT 13 LOADINGS

WELD	**** DEADWEIGHT LOAD[a] *****			****** THERMAL LOAD ******			OP PRESSURE
	AF(KIPS)	BM(IN-K)	SIG(KSI)	AF(KIPS)	BM(IN-K)	SIG(KSI)	(KSI)
1	0.	0.	0.00	-30.	21281.	10.12	2.24
2	0.	0.	0.00	0.	0.	0.00	2.24
3	0.	0.	0.00	0.	0.	0.00	2.24
4	0.	0.	0.00	-30.	3319.	1.47	2.24
5	0.	0.	0.00	-149.	9679.	2.35	2.24
6	0.	0.	0.00	-75.	6427.	1.67	2.18
7	0.	0.	0.00	-100.	5657.	1.89	2.18
8	0.	0.	0.00	-100.	6265.	2.13	2.18
9	0.	0.	0.00	-15.	1035.	.36	2.18
10	0.	0.	0.00	-15.	3563.	1.36	2.18
11	0.	0.	0.00	75.	10571.	3.46	2.18
12	0.	0.	0.00	35.	4504.	2.71	2.28
13	0.	0.	0.00	0.	0.	0.00	2.28
14	0.	0.	0.00	0.	0.	0.00	2.28
15	0.	0.	0.00	35.	4283.	2.58	2.28
16	0.	0.	0.00	30.	5221.	2.20	2.28

WELD	*********** OBE LOAD ***********				*********** SSE LOAD ***********			
	PEAK G	AF(KIPS)	BM(IN-K)	SIG(KSI)	PEAK G	AF(KIPS)	BM(IN-K)	SIG(KSI)
1	.10	358.	4231.	3.52	.15	248.	4707.	3.29
2	.10	0.	0.	0.00	.15	0.	0.	0.00
3	.10	0.	0.	0.00	.15	0.	0.	0.00
4	.10	372.	2724.	2.85	.15	257.	6427.	4.16
5	.10	372.	6466.	2.86	.15	257.	9463.	3.40
6	.10	65.	11303.	3.49	.15	120.	9183.	3.02
7	.10	65.	10716.	4.50	.15	120.	8627.	3.87
8	.10	65.	5840.	2.56	.15	120.	4295.	2.15
9	.10	65.	5860.	2.57	.15	128.	5928.	2.82
10	.10	76.	5754.	2.57	.15	124.	6493.	3.03
11	.10	75.	7843.	2.63	.15	123.	8151.	2.86
12	.10	565.	15713.	11.49	.15	368.	10101.	7.41
13	.10	0.	0.	0.00	.15	0.	0.	0.00
14	.10	0.	0.	0.00	.15	0.	0.	0.00
15	.10	587.	7353.	6.86	.15	389.	5554.	4.93
16	.10	587.	9283.	5.75	.15	389.	6171.	3.82

[a] The data are not available, but the load is negligible.

Table A-14. Geometry and loadings for sample plant 14.

PLANT 14 GEOMETRY

WELD	INNER RADIUS (INCHES)	THICKNESS (INCHES)	AREA (IN**2)	SECTION MOD (IN**3)
1	14.50	2.45	242.07	2076.58
2	14.50	2.45	242.07	2076.58
3	14.50	2.45	242.07	2076.58
4	14.50	2.45	242.07	2076.58
5	15.50	3.38	364.47	3506.69
6	15.50	3.31	357.07	3421.92
7	15.50	2.60	274.45	2513.69
8	15.50	2.60	274.45	2513.69
9	15.50	2.60	274.45	2513.69
10	15.50	2.60	274.45	2513.69
11	15.50	3.19	342.64	3258.22
12	13.75	2.32	217.34	1767.62
13	13.75	2.32	217.34	1767.62
14	13.75	2.32	217.34	1767.62
15	13.75	2.32	217.34	1767.62
16	13.75	3.03	290.62	2486.78

PLANT 14 LOADINGS

WELD	**** DEADWEIGHT LOAD *****			****** THERMAL LOAD ******			OP PRESSURE
	AF(KIPS)	BM(IN-K)	SIG(KSI)	AF(KIPS)	BM(IN-K)	SIG(KSI)	(KSI)
1	25.	581.	.38	-23.	16478.	7.84	2.24
2	15.	353.	.23	-21.	1779.	.77	2.24
3	16.	336.	.23	-21.	3588.	1.64	2.24
4	18.	218.	.18	-21.	10087.	4.77	2.24
5	23.	100.	.09	-125.	14296.	3.73	2.24
6	18.	90.	.08	-68.	5210.	1.33	2.18
7	14.	260.	.15	-75.	4300.	1.44	2.18
8	9.	233.	.13	-75.	4118.	1.36	2.18
9	2.	293.	.12	-8.	1563.	.59	2.18
10	6.	159.	.09	-8.	3558.	1.39	2.18
11	19.	272.	.14	68.	6885.	2.31	2.18
12	28.	248.	.27	12.	5977.	3.44	2.28
13	25.	251.	.26	12.	4977.	2.87	2.28
14	3.	754.	.44	12.	2610.	1.53	2.28
15	17.	489.	.35	12.	4064.	2.35	2.28
16	20.	809.	.39	10.	4671.	1.91	2.28

WELD	************ OBE LOAD ************				************ SSE LOAD ************			
	PEAK G	AF(KIPS)	BM(IN-K)	SIG(KSI)	PEAK G	AF(KIPS)	BM(IN-K)	SIG(KSI)
1	.09	369.	3874.	3.39	.20	1391.	12409.	11.72
2	.09	364.	2956.	2.93	.20	1368.	9048.	10.01
3	.09	351.	5224.	3.97	.20	1320.	15959.	13.14
4	.09	351.	5638.	4.17	.20	1302.	17246.	13.68
5	.09	234.	5678.	2.26	.20	882.	17626.	7.45
6	.09	163.	10276.	3.46	.20	367.	25029.	8.34
7	.09	108.	7503.	3.38	.20	263.	18163.	8.18
8	.09	108.	4646.	2.24	.20	242.	9134.	4.52
9	.09	134.	4382.	2.23	.20	304.	9801.	5.01
10	.09	118.	4991.	2.42	.20	269.	10159.	5.02
11	.09	110.	14544.	4.78	.20	247.	32614.	10.73
12	.09	503.	14612.	10.58	.20	1393.	42200.	30.28
13	.09	503.	12999.	9.67	.20	1393.	37536.	27.64
14	.09	520.	8731.	7.33	.20	1443.	25281.	20.94
15	.09	520.	4666.	5.03	.20	1447.	13621.	14.36
16	.09	481.	5882.	4.02	.20	1342.	16993.	11.45

Table A-15. Geometry and loadings for sample plan 15.

PLANT 15 GEOMETRY

WELD	INNER RADIUS (INCHES)	THICKNESS (INCHES)	AREA (IN**2)	SECTION MOD (IN**3)
1	14.50	2.45	242.07	2076.56
2	14.50	2.45	242.07	2076.58
3	14.50	2.99	300.49	2674.14
4	14.50	2.99	300.49	2674.14
5	15.50	3.38	364.47	3506.69
6	15.50	3.31	357.07	3421.92
7	15.50	2.60	274.45	2513.69
8	15.50	2.60	274.45	2513.69
9	15.50	2.60	274.45	2513.69
10	15.50	2.60	274.45	2513.69
11	15.50	3.19	342.64	3258.22
12	13.75	2.32	217.34	1767.62
13	13.75	2.32	217.34	1767.62
14	13.75	2.32	217.34	1767.62
15	13.75	2.32	217.34	1767.62
16	13.75	3.03	290.62	2486.78

PLANT 15 LOADINGS

WELD	**** DEADWEIGHT LOAD *****			****** THERMAL LOAD ******			OP PRESSURE
	AF(KIPS)	BM(IN-K)	SIG(KSI)	AF(KIPS)	BM(IN-K)	SIG(KSI)	(KSI)
1	0.	61.	.03	7.	29203.	14.09	2.24
2	0.	0.	0.00	0.	0.	0.00	2.24
3	0.	0.	0.00	0.	0.	0.00	2.24
4	0.	217.	.08	7.	14186.	5.33	2.24
5	9.	431.	.15	206.	25454.	7.82	2.24
6	5.	295.	.10	99.	6608.	2.21	2.18
7	18.	166.	.13	120.	5465.	2.61	2.18
8	13.	155.	.11	120.	5857.	2.77	2.18
9	0.	205.	.08	7.	951.	.40	2.18
10	0.	248.	.10	7.	3973.	1.61	2.18
11	18.	399.	.17	120.	10801.	3.67	2.18
12	0.	240.	.14	10.	9064.	5.17	2.28
13	0.	0.	0.00	0.	0.	0.00	2.28
14	0.	0.	0.00	0.	0.	0.00	2.28
15	0.	183.	.10	10.	7602.	4.35	2.28
16	0.	132.	.05	12.	8112.	3.30	2.28

WELD	*********** OBE LOAD ***********				*********** SSE LOAD ***********			
	PEAK G	AF(KIPS)	BM(IN-K)	SIG(KSI)	PEAK G	AF(KIPS)	BM(IN-K)	SIG(KSI)
1	.08	138.	1860.	1.47	.15	275.	3720.	2.93
2	.08	0.	0.	0.00	.15	0.	0.	0.00
3	.08	0.	0.	0.00	.15	0.	0.	0.00
4	.08	94.	1835.	1.00	.15	188.	3670.	2.00
5	.08	94.	1835.	.78	.15	188.	3670.	1.56
6	.08	65.	2710.	.97	.15	130.	5420.	1.95
7	.08	65.	2710.	1.31	.15	130.	5420.	2.63
8	.08	65.	2710.	1.31	.15	130.	5420.	2.63
9	.08	29.	2955.	1.28	.15	58.	5910.	2.56
10	.08	29.	2955.	1.28	.15	58.	5910.	2.56
11	.08	29.	2955.	.99	.15	58.	5910.	1.98
12	.08	76.	2095.	1.53	.15	152.	4190.	3.07
13	.08	0.	0.	0.00	.15	0.	0.	0.00
14	.08	0.	0.	0.00	.15	0.	0.	0.00
15	.08	69.	1935.	1.41	.15	137.	3870.	2.82
16	.08	69.	1935.	1.02	.15	137.	3870.	2.03

Table A-16. Geometry and loadings for sample plant 16.

PLANT 16 GEOMETRY

WELD	INNER RADIUS (INCHES)	THICKNESS (INCHES)	AREA (IN**2)	SECTION MOD (IN**3)
1	14.50	2.45	242.07	2076.58
2	14.50	2.45	242.07	2076.58
3	14.50	2.99	300.49	2674.14
4	14.50	2.99	300.49	2674.14
5	15.50	3.38	364.47	3506.69
6	15.50	3.31	357.07	3421.92
7	15.50	2.60	274.45	2513.69
8	15.50	2.60	274.45	2513.69
9	15.50	2.60	274.45	2513.69
10	15.50	2.60	274.45	2513.69
11	15.50	3.19	342.64	3258.22
12	13.75	2.32	217.34	1767.62
13	13.75	2.32	217.34	1767.62
14	13.75	2.32	217.34	1767.62
15	13.75	2.32	217.34	1767.62
16	13.75	3.03	290.62	2486.78

PLANT 16 LOADINGS

WELD	**** DEADWEIGHT LOAD *****			****** THERMAL LOAD ******			OP PRESSURE
	AF(KIPS)	BM(IN-K)	SIG(KSI)	AF(KIPS)	BM(IN-K)	SIG(KSI)	(KSI)
1	9.	286.	.17	10.	30983.	14.96	2.24
2	0.	0.	0.00	0.	0.	0.00	2.24
3	0.	0.	0.00	0.	0.	0.00	2.24
4	4.	121.	.06	10.	14162.	5.33	2.24
5	11.	216.	.09	-200.	26376.	6.97	2.24
6	23.	204.	.12	-90.	6265.	1.58	2.18
7	18.	82.	.10	-100.	5430.	1.80	2.18
8	12.	67.	.07	-100.	5958.	2.01	2.18
9	1.	280.	.12	-10.	1083.	.39	2.18
10	4.	223.	.10	-10.	4019.	1.56	2.18
11	21.	273.	.15	90.	10281.	3.42	2.18
12	10.	290.	.21	2.	9616.	5.45	2.28
13	0.	0.	0.00	0.	0.	0.00	2.28
14	0.	0.	0.00	0.	0.	0.00	2.28
15	9.	179.	.14	2.	9231.	5.23	2.28
16	11.	384.	.19	2.	10856.	4.37	2.28

WELD	*********** OBE LOAD ***********				*********** SSE LOAD ***********			
	PEAK G	AF(KIPS)	BM(IN-K)	SIG(KSI)	PEAK G	AF(KIPS)	BM(IN-K)	SIG(KSI)
1	.13	824.	16584.	11.39	.25	1333.	11690.	11.14
2	.13	0.	0.	0.00	.25	0.	0.	0.00
3	.13	0.	0.	0.00	.25	0.	0.	0.00
4	.13	824.	16442.	8.89	.25	1225.	19027.	11.19
5	.13	824.	25545.	9.55	.25	1225.	19027.	8.79
6	.13	199.	20636.	6.59	.25	68.	9996.	3.11
7	.13	199.	14912.	6.66	.25	68.	9996.	4.22
8	.13	199.	10113.	4.75	.25	68.	9996.	4.22
9	.13	199.	12218.	5.59	.25	88.	6082.	2.74
10	.13	199.	12076.	5.53	.25	88.	6082.	2.74
11	.13	199.	13492.	4.72	.25	88.	6082.	2.12
12	.13	368.	19734.	12.86	.25	636.	13348.	10.48
13	.13	0.	0.	0.00	.25	0.	0.	0.00
14	.13	0.	0.	0.00	.25	0.	0.	0.00
15	.13	368.	15264.	10.33	.25	736.	12937.	10.71
16	.13	368.	17951.	8.48	.25	736.	12937.	7.73

Table A-17. Geometry and loadings for sample plant 17.

PLANT 17 GEOMETRY

WELD	INNER RADIUS (INCHES)	THICKNESS (INCHES)	AREA (IN**2)	SECTION MOD (IN**3)
1	14.50	2.45	242.07	2076.58
2	14.50	2.45	242.07	2076.58
3	14.50	2.99	300.49	2674.14
4	14.50	2.99	300.49	2674.14
5	15.50	3.38	364.47	3506.69
6	15.50	3.31	357.07	3421.92
7	15.50	2.60	274.45	2513.69
8	15.50	2.60	274.45	2513.69
9	15.50	2.60	274.45	2513.69
10	15.50	2.60	274.45	2513.69
11	15.50	3.19	342.64	3258.22
12	13.75	2.32	217.34	1767.62
13	13.75	2.32	217.34	1767.62
14	13.75	2.32	217.34	1767.62
15	13.75	2.32	217.34	1767.62
16	13.75	3.03	290.62	2486.78

PLANT 17 LOADINGS

WELD	**** DEADWEIGHT LOAD *****			****** THERMAL LOAD ******			OP PRESSURE
	AF(KIPS)	BM(IN-K)	SIG(KSI)	AF(KIPS)	BM(IN-K)	SIG(KSI)	(KSI)
1	22.	1055.	.60	47.	19669.	9.67	2.24
2	7.	818.	.42	29.	419.	.32	2.24
3	22.	226.	.16	28.	9955.	3.82	2.24
4	23.	81.	.11	28.	11224.	4.29	2.24
5	29.	854.	.32	140.	17153.	5.28	2.24
6	21.	236.	.13	98.	7032.	2.33	2.18
7	16.	179.	.13	116.	5325.	2.54	2.18
8	11.	133.	.09	116.	5378.	2.56	2.18
9	2.	214.	.09	3.	1361.	.55	2.18
10	3.	172.	.08	3.	3463.	1.39	2.18
11	15.	255.	.12	116.	9820.	3.35	2.18
12	25.	900.	.62	24.	5239.	3.07	2.28
13	22.	196.	.21	24.	3899.	2.32	2.26
14	3.	806.	.47	25.	1607.	1.02	2.28
15	15.	605.	.41	21.	4233.	2.49	2.28
16	18.	1064.	.49	18.	3911.	1.63	2.28

WELD	*********** OBE LOAD ***********				*********** SSE LOAD ***********			
	PEAK G	AF(KIPS)	BM(IN-K)	SIG(KSI)	PEAK G	AF(KIPS)	BM(IN-K)	SIG(KSI)
1	.06	150.	5686.	3.36	.12	177.	4788.	3.04
2	.06	150.	1473.	1.33	.12	176.	1384.	1.39
3	.06	144.	3029.	1.61	.12	172.	2798.	1.62
4	.06	144.	3153.	1.66	.12	172.	2924.	1.67
5	.06	144.	4457.	1.67	.12	172.	5309.	1.99
6	.06	244.	13990.	4.77	.12	200.	11680.	3.97
7	.06	248.	9823.	4.81	.12	202.	8216.	4.00
8	.06	250.	4544.	2.72	.12	205.	3892.	2.30
9	.06	253.	2393.	1.87	.12	207.	1976.	1.54
10	.06	254.	3517.	2.32	.12	208.	2929.	1.92
11	.06	256.	22060.	7.52	.12	209.	18[illegible]9.	6.16
12	.06	437.	11335.	8.42	.12	355.	9258.	6.87
13	.06	438.	10060.	7.71	.12	357.	8179.	6.27
14	.06	455.	7591.	6.39	.12	369.	6199.	5.20
15	.06	460.	7335.	6.27	.12	374.	5997.	5.11
16	.06	460.	11354.	6.15	.12	374.	9265.	5.01

NRC FORM 335 (2-84) NRCM 1102, 3201, 3202

U.S. NUCLEAR REGULATORY COMMISSION

BIBLIOGRAPHIC DATA SHEET

SEE INSTRUCTIONS ON THE REVERSE

1. REPORT NUMBER (Assigned by TIDC, add Vol. No., if any)
NUREG/CR-3660, Vol. 2
UCID-19988

2. TITLE AND SUBTITLE
Probability of Pipe Failure in the Reactor Coolant Loops of Westinghouse PWR Plants
Vol. 2: Pipe Failure Induced by Crack Growth

3. LEAVE BLANK

4. DATE REPORT COMPLETED

MONTH	YEAR
January	1984

5. AUTHOR(S)
H.H. Woo, R.W. Mensing, B.J. Benda

6. DATE REPORT ISSUED

MONTH	YEAR
August	1984

7. PERFORMING ORGANIZATION NAME AND MAILING ADDRESS (Include Zip Code)
Lawrence Livermore National Laboratory
P.O. Box 808, L-46
Livermore, CA 94550

8. PROJECT/TASK/WORK UNIT NUMBER

9. FIN OR GRANT NUMBER
A0133

10. SPONSORING ORGANIZATION NAME AND MAILING ADDRESS (Include Zip Code)
Division of Engineering Technology
Office of Nuclear Regulatory Research
U.S. Nuclear Regulatory Commission
Washington, DC 20555

11a. TYPE OF REPORT
Technical

b. PERIOD COVERED (Inclusive dates)

12. SUPPLEMENTARY NOTES

13. ABSTRACT (200 words or less)

This report assesses the probability of reactor coolant loop (RCL) piping failures resulting from a crack growth mechanism. The Westinghouse pressurized water reactor (PWR) plants in the United States east of the Rocky Mountains are considered. After the introduction (Section 1), the assessment is presented in five parts (Sections 2-6). Section 2 describes the characteristics of RCL piping in these Westinghouse PWR plants. Section 3 describes the methodology used in the analysis. Sections 4 and 5 present the best-estimate and uncertainty analyses, respectively. Our conclusions are presented in Section 6, along with recommended items for consideration in future licensing regulations.

14. DOCUMENT ANALYSIS – a. KEYWORDS/DESCRIPTORS

reactor coolant loops
Westinghouse pressurized water reactor

b. IDENTIFIERS/OPEN-ENDED TERMS

15. AVAILABILITY STATEMENT
Unlimited

16. SECURITY CLASSIFICATION
(This page)
Unclassified
(This report)
Unclassified

17. NUMBER OF PAGES

18. PRICE

UNITED STATES
NUCLEAR REGULATORY COMMISSION
WASHINGTON, D.C. 20555

OFFICIAL BUSINESS
PENALTY FOR PRIVATE USE, $300

FOURTH CLASS MAIL
POSTAGE & FEES PAID
USNRC
WASH. D. C.
PERMIT No. G 67

NUREG/CR-3660, Vol. 2 Probability of Pipe Failure in the Reactor Coolant Loops of Westinghouse PWR Plants AUGUST 1984

120555078877 1 LAN1RM
US NRC
ADM-DIV OF TIDC
POLICY & PUB MGT BR-PDR NUREG
W-501
WASHINGTON DC 20555